# FROM PRESTELLAR CORES TO PROTOSTARS: THE INITIAL CONDITIONS OF STAR FORMATION

PHILIPPE ANDRÉ
*CEA/DSM/DAPNIA, Service d'Astrophysique, Saclay, France*

DEREK WARD-THOMPSON
*University of Wales at Cardiff*

and

MARY BARSONY
*University of California at Riverside*

The last decade has witnessed significant advances in our observational understanding of the earliest stages of low-mass star formation. The advent of sensitive receivers on large radio telescopes such as the James Clerk Maxwell Telescope (JCMT) and Institut de Radio Astronomie Millimétrique (IRAM) 30m telescope has led to the identification of young protostars at the beginning of the main accretion phase ("Class 0" objects) and has made it possible for the first time to probe the inner density structure of precollapse cores. Class 0 objects are characterized by strong, centrally condensed dust continuum emission at submillimeter wavelengths, very little emission shortward of $\sim$10 $\mu$m, and powerful jetlike outflows. Direct evidence for gravitational infall has been observed in several of them. They are interpreted as accreting protostars that have not yet accumulated the majority of their final stellar mass. In contrast to protostars, prestellar cores have flat inner density profiles, suggesting that the initial conditions for fast protostellar collapse depart sometimes significantly from a singular isothermal sphere. In the case of nonsingular initial conditions, the beginning of protostellar evolution is expected to feature a brief phase of vigorous accretion and ejection, which may coincide with Class 0 objects. In addition, submillimeter continuum imaging surveys of regions of multiple star formation, such as Ophiuchus and Serpens, suggest a picture according to which each star in an embedded cluster is built from a finite reservoir of mass and the associated initial mass function (IMF) is primarily determined at the prestellar stage of evolution.

## I. INTRODUCTION

The formation of low-mass stars is believed to involve a series of conceptually different stages (e.g., Larson 1969; Shu et al. 1987). The first stage corresponds to the fragmentation of a molecular cloud into a number of gravitationally bound cores, which are initially supported against

gravity by a combination of thermal, magnetic, and turbulent pressures (e.g., Mouschovias 1991; Shu et al. 1987). These prestellar condensations or fragments form and evolve as a result of a still poorly understood mechanism that may involve ambipolar diffusion (e.g., Mouschovias 1991), the dissipation of turbulence (e.g., Nakano 1998), and an outside impulse (e.g., Bonnell et al. 1997). Once such a condensation becomes gravitationally unstable and collapses, the main *theoretical* features of the ensuing dynamical evolution have been known since the pioneering work of Larson (1969). During a probably brief initial phase, the released gravitational energy is freely radiated away, and the collapsing fragment stays roughly isothermal. This "runaway" isothermal collapse phase tends to produce a strong central concentration of matter with a radial density gradient approaching $\rho \propto r^{-2}$ at small radii essentially independently of initial conditions (e.g., Whitworth and Summers 1985; Blottiau et al. 1988; Foster and Chevalier 1993). It ends with the formation of an opaque, hydrostatic protostellar object in the center (e.g., Larson 1969; Boss and Yorke 1995; Bate 1998). Numerical simulations in fact predict the successive formations of two hydrostatic objects, one before and one after the dissociation of molecular hydrogen (see Boss and Yorke 1995), but we will not distinguish between them here. The system then enters the main accretion phase, during which the central object builds up its mass ($M_\star$) from a surrounding infalling envelope (of mass $M_{\rm env}$) and accretion disk, while progressively warming up. In this chapter, we will refer to the system consisting of the central object plus envelope and disk as an accreting protostar. The youngest accreting protostars have $M_{\rm env} \gg M_\star$ and radiate the accretion luminosity $L_{\rm acc} \approx GM_\star \dot{M}_{\rm acc}/R_\star$. In the "standard" theory of isolated star formation (Shu et al. 1987, 1993), the collapse initial conditions are taken to be (static) singular isothermal spheroids ($\rho \sim (a^2/2\pi G)\, r^{-2}$, cf. Li and Shu 1996, 1997), there is no runaway collapse phase, and the accretion rate $\dot{M}_{\rm acc}$ is constant in time $\sim a^3/G$, where $a$ is the effective isothermal sound speed. With other collapse initial conditions, the accretion rate is generally time dependent (see section III.D below).

Observations have shown that the main accretion phase is always accompanied by a powerful ejection of a small fraction of the accreted material in the form of prominent bipolar jets or outflows (e.g., Bachiller 1996). These outflows are believed to carry away the excess angular momentum of the infalling matter (e.g., the chapter by Königl and Pudritz, this volume). When the central object has accumulated most ($\gtrsim$90%) of its final, main-sequence mass, it becomes a pre-main-sequence (PMS) star, which evolves approximately at fixed mass on the Kelvin-Helmholtz contraction timescale (e.g., Stahler and Walter 1993). (Note that, during the protostellar accretion phase, stars more massive than a few 0.1 $M_\odot$ start burning deuterium whereas stars with masses in excess of $\sim$8 $M_\odot$ begin to burn hydrogen; see Palla and Stahler 1991.)

The details of the earliest stages outlined above are still poorly known. Improving our understanding of these early stages is of prime importance since to some extent they must govern the origin of the stellar initial mass function (IMF).

Observationally, it is by comparing the structure of starless dense cores with that of the envelopes surrounding the youngest stellar objects that one may hope to estimate the initial conditions for protostellar collapse. The purpose of this chapter is to review several major advances made in this field over the last decade, thanks mostly to ground-based (sub)millimeter continuum observations. We discuss results obtained on prestellar cores and young accreting protostars in sections II and III, respectively. We then combine these two sets of results and conclude in section IV.

## II. PRESTELLAR CORES

### A. Definition and Identification

The prestellar stage of star formation may be defined as the phase in which a gravitationally bound core has formed in a molecular cloud and evolves toward higher degrees of central condensation, but no central hydrostatic protostellar object exists yet within the core.

A pioneering survey of isolated dense cores in dark clouds was carried out in transitions of $NH_3$ by Myers and coworkers (see Myers and Benson 1983; Benson and Myers 1989, and references therein), who cataloged about 90 cores. These were separated into starless cores and cores with stars (Beichman et al. 1986), on the basis of the presence or absence of an embedded source detected by the *Infrared Astronomy Satellite* (IRAS). The starless $NH_3$ cores were identified by Beichman et al. as the potential sites of future isolated low-mass star formation. Other dense core surveys have been carried out by Clemens and Barvainis (1988), Wood et al. (1994), Bourke et al. (1995*a*,*b*), Lee and Myers (1999), and Jessop and Ward-Thompson (1999).

Using the 15-m James Clerk Maxwell Telescope (JCMT), Ward-Thompson et al. (1994) observed the 800-$\mu$m dust continuum emission from about 20 starless $NH_3$ cores from the Benson and Myers list, mapping four of the cores, and showed that they have larger full-width at half maximum (FWHM) sizes than, but comparable masses to, the envelopes of the youngest protostars (Class 0 sources; see section III below). This is consistent with starless $NH_3$ cores being prestellar in nature and the precursors of protostars (see also Mizuno et al. 1994). Ward-Thompson et al. also demonstrated that prestellar cores do not have density profiles which can be modeled by a single scale-free power law; instead they have flat inner radial density profiles, suggestive of magnetically supported cores contracting by ambipolar diffusion (see Mouschovias 1991, 1995,

and references therein). Recent molecular line spectroscopy of several prestellar cores (e.g., Tafalla et al. 1998 and the chapter by Myers et al., this volume) appears to support the argument that they are contracting, but more slowly than the infall seen toward Class 0 protostars (e.g., Mardones et al. 1997; see section III.C).

The 800-$\mu$m study by Ward-Thompson et al. (1994) also suggests that wide-field submillimeter continuum imaging may be a powerful tool for searching for new prestellar cores in the future (cf. Ristorcelli et al. 1998).

## B. Spectral Energy Distributions and Temperatures

The advent of the *Infrared Space Observatory* (ISO) of the European Space Agency (ESA) has allowed prestellar cores to be studied in the

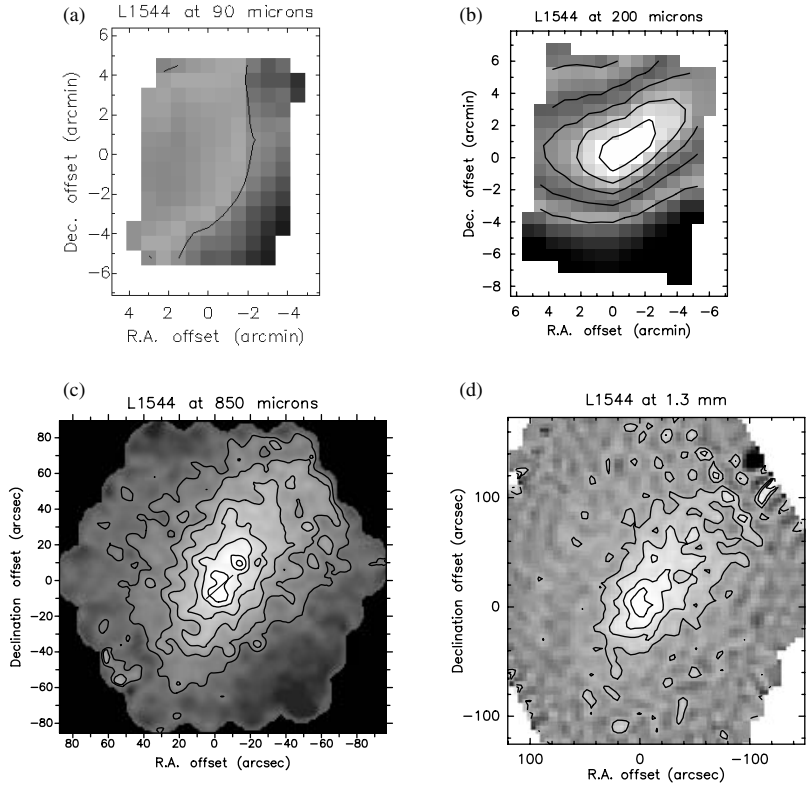


Figure 1. Dust continuum images of L1544 at 90 $\mu$m (a) and 200 $\mu$m (b) from ISOPHOT, at 850 $\mu$m (c) from SCUBA, and at 1.3 mm (d) from the IRAM 30 m. A polarization **E**-vector, perpendicular to the **B** field, is overlaid on the 850 $\mu$m image (c), as measured with the SCUBA polarimeter. The observed morphology is consistent with a magnetically supported core that has flattened along the direction of the mean magnetic field.

far-infrared (FIR) for the first time (Ward-Thompson and André, in prep.), since these cores were not detected by IRAS. Likewise, the Submillimetre Common User Bolometer Array (SCUBA) camera on the JCMT has allowed prestellar cores to be observed in the submillimeter region with a greater signal-to-noise ratio than ever before (Ward-Thompson et al., in prep.). Prestellar cores emit almost all of their radiation in the FIR and submillimeter regimes, so the combination of these two instruments provides a unique opportunity to study them.

As an illustration, Fig. 1 shows a series of images of the L1544 prestellar core at 90 and 200 $\mu$m (from ISO), 850 $\mu$m (from SCUBA), and 1.3 mm (from IRAM). The core is clearly detected at 200–1300 $\mu$m but is almost undetected at 90 $\mu$m. This shows that the core is very cold, and its dust temperature can be obtained from fitting a modified black body to the observed emission. The spectral energy distribution (SED) of L1544 in the FIR and submillimeter wavelength regimes is shown in Fig. 2. The solid line is a gray-body curve of the form

$$S_\nu = B_\nu(T_{\rm dust})\,[1 - \exp(-\tau_\nu)]\,\Delta\Omega$$

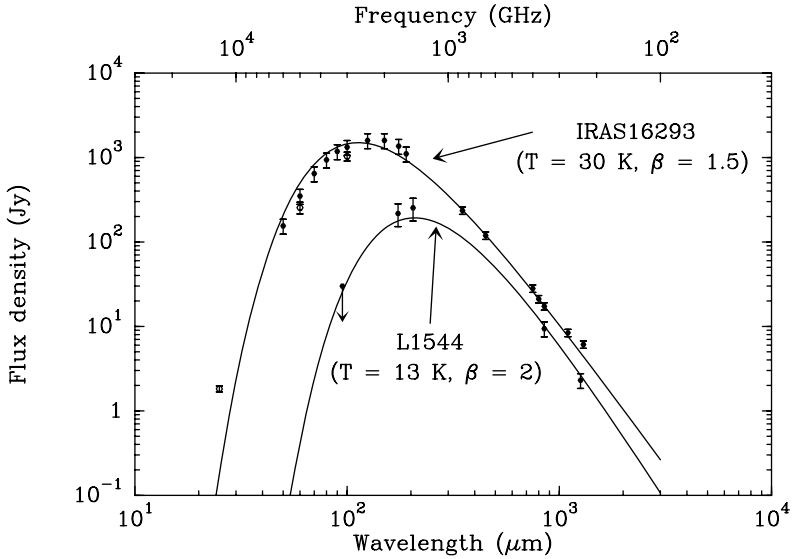


Figure 2. Spectral energy distributions of the prestellar core L1544 and the Class 0 protostar IRAS 16293, along with gray-body fits (see text). The L1544 SED is based on ISOPHOT, JCMT, and IRAM data from Ward-Thompson et al. (in prep.) The IRAS 16293 SED is based on IRAS, ISO-LWS (Correia et al., in prep.; see also Ceccarelli et al. 1998), and JCMT data (Sandell 1994). The fits suggest that both sources are opaque ($\tau_\nu > 1$) at $\lambda < 30$–$50$ $\mu$m. Note that a simple gray-body model cannot account for the 25-$\mu$m emission of IRAS 16293 and that a two-component model is required (Correia, in prep.).

where $B_\nu(T_{\rm dust})$ is the Planck function at frequency $\nu$ for a dust temperature $T_{\rm dust}$, $\tau_\nu = \kappa_\nu \Sigma$ is the dust optical depth through a mass column density $\Sigma$ (see below), and $\Delta\Omega$ is the source solid angle. In this simple modeling, the dust opacity per unit (gas + dust) mass column density, $\kappa_\nu$, is assumed to scale as $\nu^\beta$, with $\beta = 1.5$–2, as usually appropriate in the submillimeter range (e.g., Hildebrand 1983). For L1544, a good fit to the SED is obtained with $T_{\rm dust} = 13$ K, $\beta = 2$, $\tau_\nu = 0.12$ at $\lambda = 100$ $\mu$m, and $\Delta\Omega = 2.3 \times 10^{-7}$ sr. Similar results are obtained in other starless cores. This confirms the lack of any warm dust in such cores and consequently the lack of any embedded protostellar object. The (sub)millimeter data show a morphology similar to the ISO images at much higher resolution, indicating that the same dust is being observed at all wavelengths. Consequently the temperature derived from the SED is representative of all the emitting dust and can be used to convert submillimeter fluxes into estimates of dust masses and, hence, to gas masses.

### C. Mass and Density Structure

Dust emission is generally optically thin at (sub)millimeter wavelengths and hence is a direct tracer of the mass content of molecular cloud cores. For an isothermal dust source, the total (gas + dust) mass $M(r < R)$ contained within a radius $R$ from the center is related to the submillimeter flux density $S_\nu(\theta)$ integrated over a circle of projected angular radius $\theta = R/d$ by

$$M(r < R) \equiv \pi R^2 \langle \Sigma \rangle_R = [S_\nu(\theta)\, d^2]/[\kappa_\nu\, B_\nu(T_{\rm dust})],$$

where $\langle \Sigma \rangle_R$ is the average mass column density. The dust opacity $\kappa_\nu$ is somewhat uncertain, but the uncertainties are much reduced when appropriate dust models are used (see Henning et al. 1995 for a review). For prestellar cores of intermediate densities ($n_{\rm H_2} \lesssim 10^5$ cm$^{-3}$), $\kappa_\nu$ is believed to be close to $\kappa_{1.3} = 0.005$ cm$^2$ g$^{-1}$ at 1.3 mm (e.g., Hildebrand 1983; Preibisch et al. 1993). In denser cloud cores and protostellar envelopes, grain coagulation and the formation of ice mantles make $\kappa_\nu$ a factor of $\sim$2 larger, i.e., $\kappa_{1.3} = 0.01$ cm$^2$ g$^{-1}$ assuming a gas-to-dust mass ratio of 100 (e.g., Ossenkopf and Henning 1994). A still higher value, $\kappa_{1.3} = 0.02$ cm$^2$ g$^{-1}$, is recommended in protoplanetary disks (Beckwith et al. 1990; Pollack et al. 1994).

Following this method, FWHM masses ranging from $\sim$0.5 $M_\odot$ to $\sim$35 $M_\odot$ are derived for the nine isolated cores mapped by Ward-Thompson et al. (1999).

Although observed prestellar cores are generally not circularly or elliptically symmetric (see, e.g., Fig. 1), one can still usefully constrain their radial density profiles by averaging the (sub)millimeter emission in circular or elliptical annuli.

Figure 3a shows the azimuthally averaged radial intensity profile of the prestellar core L1689B at 1.3 mm, compared to the profile of a spherical

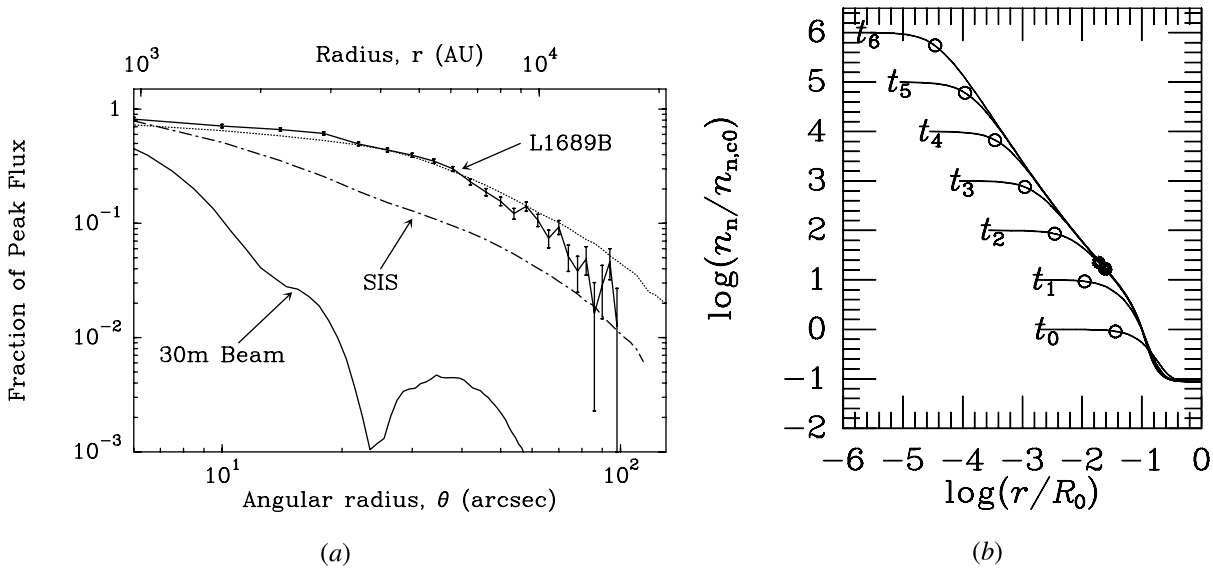


Figure 3. (a) (left) Radial intensity profile of L1689B at 1.3 mm, illustrating that prestellar cores have flat inner density profiles (from André et al. 1996). For comparison, the dotted curve shows a spherical isothermal model with $\rho(r) \propto r^{-1.2}$ for $r < 4000$ AU and $\rho(r) \propto r^{-2}$ for $r \geq 4000$ AU. The dash-dotted curve shows a model with $\rho(r) \propto r^{-2}$, such as a singular isothermal sphere (SIS). (b) (right) Typical density profiles expected for a magnetically supported core undergoing ambipolar diffusion at various times increasing from $t_0$ to $t_6$ (from Ciolek and Mouschovias 1994). The normalization values are $n_{n,c0} = 2.6 \times 10^3$ cm$^{-3}$ and $R_0 = 4.29$ pc. Open circles mark the instantaneous radius of the uniform-density central region; starred circles mark the radius of the magnetically supercritical region (present only for $t \geq t_2$).

isothermal core model with $\rho(r) \propto r^{-2}$. The model intensity profile results from a complete simulation that takes into account both the observing technique (dual-beam mapping) and the reduction method (cf. André et al. 1996). We see that L1689B exhibits the familiar radial profile of prestellar cores, with a flat inner region, steepening toward the edges (Ward-Thompson et al. 1994; André et al. 1996; Ward-Thompson et al. 1999). In this representative example, the radial density profile inferred under the assumption of a constant dust temperature is as flat as $\rho(r) \propto r^{-0.4}$ (if the 3-D core shape is disklike) or $\rho(r) \propto r^{-1.2}$ (if the core shape is spheroidal) at radii less than $R_{\rm flat} \sim 4000$ AU and approaches $\rho(r) \propto r^{-2}$ only between $\sim$4000 AU and $\sim$15,000 AU.

More recently, it has been possible to constrain the outer density gradient of starless cores through absorption studies in the mid-infrared with the camera aboard ISO (ISOCAM) (e.g., Abergel et al. 1996, 1998; Bacmann et al. 1998). It appears that isolated prestellar cores are often characterized by sharp edges, steeper than $\rho \propto r^{-3}$ or $\rho \propto r^{-4}$, at radii $R \gtrsim 15{,}000$ AU.

These features of prestellar density structure (i.e., inner flattening and sharp outer edge) are qualitatively consistent with models of magnetically supported cores evolving through ambipolar diffusion prior to protostar formation (see Fig. 3b; e.g., Ciolek and Mouschovias 1994; Basu and Mouschovias 1995), although the models generally require fairly strong magnetic fields ($\sim$100 $\mu$G). Alternatively, the observed structure may also be explained by models of thermally supported self-gravitating cores interacting with an external UV radiation field (e.g., Falgarone and Puget 1985; Chièze and Pineau des Forêts 1987).

### D. Lifetimes

Beichman et al. (1986) used the ratio of numbers of starless cores to numbers of cores with embedded IRAS sources to estimate their relative timescales. They found roughly equal numbers of cores with and without IRAS sources. They estimated the lifetime of the stage of cores with stars, based on T Tauri lifetimes and pre-main-sequence HR diagram tracks (e.g., Stahler 1988). Based on this, they estimated the lifetime of the prestellar core phase to be a few times $10^6$ yr.

However, the lifetime of a prestellar core depends on its central density. Figure 4 (taken from Jessop and Ward-Thompson 1999) shows the estimated lifetime of starless cores for each of six dark cloud surveys mentioned in section II.A above, versus the mean volume density of cores in each sample. The lifespan of cores without stars in each sample was estimated from the fraction of cores with IRAS sources, using the same method as Beichman et al. (1986). An anticorrelation between lifetime and density is clearly apparent in Fig. 4. The solid line has the form $t \propto \rho^{-0.75}$, while the dashed line is of the form $t \propto \rho^{-0.5}$. These two forms are expected for cores evolving on the ambipolar diffusion timescale $t_{\rm AD} \propto x_e$ (where $x_e$ is the ionization fraction, e.g., Nakano 1984), if the dominant ionization mechanism is UV ionization or cosmic ray ionization respec-

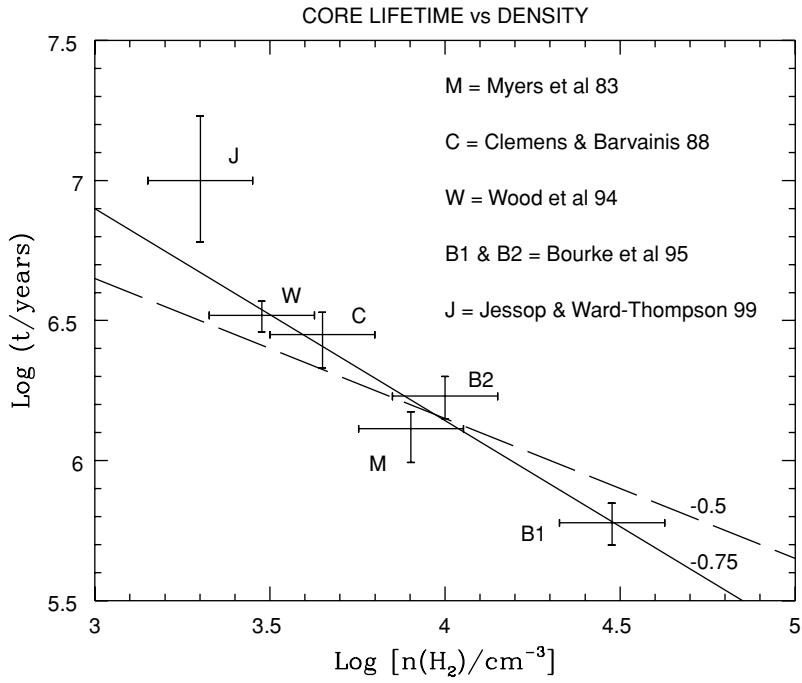


Figure 4. Plot of lifetime vs. mean density for six core samples compared with $t \propto \rho^{-0.75}$ and $t \propto \rho^{-0.5}$ as predicted by ambipolar diffusion models with different ionization mechanisms (Jessop and Ward-Thompson 1999).

tively (e.g., McKee 1989). Although the shape of the $t$ vs $\rho$ correlation is roughly consistent with expectations, Lee and Myers (1999) note that the lifetimes of cores at $n_{\mathrm{H}_2} \sim 10^4$ cm$^{-3}$ tend to be shorter than the predictions of ambipolar diffusion models by a factor $\gtrsim$3.

More details about the evolution of prestellar cores at higher densities can be inferred from the results of the submillimeter continuum SCUBA survey of Ward-Thompson et al. (in prep.). In this survey, 17 of the 38 $NH_3$ cores without IRAS sources from Benson and Myers (1989) were detected by SCUBA at 850 $\mu$m. Ward-Thompson et al. estimate that the 17 SCUBA detections all have central densities between $\sim 10^5$ and $\sim 10^6$ cm$^{-3}$, whereas the 21 nondetections must have lower central densities, typically between $\sim 10^4$ and $\sim 10^5$ cm$^{-3}$ (see Benson and Myers 1989; Butner et al. 1995, and references therein). Consequently, they deduce that the lifetime of these two phases, that of central density increasing from $\sim 10^4$ to $\sim 10^5$ cm$^{-3}$ and that of central density of $\sim 10^5$ cm$^{-3}$ until the formation of a protostellar object at the center, must be roughly equal. This result can be compared with the predictions of ambipolar diffusion models.

Figure 3b is taken from Ciolek and Mouschovias (1994) and shows the radial density profile predicted by an ambipolar diffusion model at different evolutionary stages ($t_0$ to $t_6$). The stage at which the central density

is $\sim 10^4$ cm$^{-3}$ corresponds to time $t_1$, and the stage at which the central density is $\sim 10^5$ cm$^{-3}$ corresponds to time $t_2$. The time at which a protostellar object forms is effectively $t_6$. In this model the time taken to go from $t_1$ to $t_2$ ($\sim 2 \times 10^6$ yr) is six times longer than the time taken to go from $t_2$ to $t_6$. Some discrepancy could perhaps be accounted for by the statistical errors associated with our source number counting technique, but the ratio between the two timescales should be fairly robust. The model predicts that SCUBA should only have detected one-seventh of the cores, whereas it detected half of the sample.

We are left with the conclusion that cores at central densities $\sim 10^5$ cm$^{-3}$ evolve more slowly than ambipolar diffusion models predict, a trend opposite to that noted at low densities. These departures from models involving only a static magnetic field are perhaps due to turbulence, which generates nonstatic fields and modifies core support (e.g., Gammie and Ostriker 1996; Nakano 1998; Balsara et al. 1998).

### E. Prestellar Condensations in Star-Forming Clusters

In regions of multiple star formation, submillimeter dust continuum mapping has revealed a wealth of small-scale cloud fragments, sometimes organized along filaments [e.g., Mezger et al. 1992; André et al. 1993; Casali et al. 1993; Launhardt et al. 1996; Chini et al. 1997*b*; Johnstone and Bally 1999]. Such fragmentation along filaments has not been observed in Taurus, but examples do exist in young embedded clusters forming primarily low-mass stars like $\rho$ Ophiuchi (Motte et al. 1998). The individual fragments, which are denser ($\langle n \rangle \gtrsim 10^6$–$10^7$ cm$^{-3}$) and more compact (a few thousand AU in size) than the isolated prestellar cores discussed above, often remained totally undetected (in emission) by IRAS or ISO in the mid- to far-IR. Since molecules tend to freeze out onto dust grains at low temperatures and high densities, (sub)millimeter dust emission may be the most effective tracer of such condensations (e.g., Mauersberger et al. 1992).

The most centrally condensed of these starless fragments have been claimed to be isothermal protostars: collapsing condensations with no central hydrostatic object (see section I) (e.g., Mezger et al. 1992; Launhardt et al. 1996; Motte et al. 1998). Good examples are FIR 3 and FIR 4 in NGC 2024, OphA-SM1 and OphE-MM3 in $\rho$ Oph, LBS 17-SM in Orion B, and MMS1 and MMS4 in OMC-3. This isothermal protostar interpretation remains to be confirmed, however, by observations of appropriate spectral line signatures (cf. the chapter by Myers et al. this volume).

Furthermore, the advent of large-format bolometer arrays now makes possible systematic studies of the genetic link between prestellar cloud fragments and young stars. Color Plate 3 is a 1.3-mm continuum wide-field mosaic of the $\rho$ Oph cloud (Motte et al. 1998), showing a total of 100 structures with characteristic angular scales of $\sim 15''$–$30''$ (i.e., $\sim$2000–4000 AU), which are associated with 59 starless condensations (undetected by ISO in the mid-IR) and 41 embedded young stellar objects (YSOs) (detected at IR or radio continuum wavelengths).

Comparison of the masses derived from the 1.3 mm continuum (from $\sim$0.05 $M_\odot$ to $\sim$3 $M_\odot$) with Jeans masses suggests that most of the 59 starless fragments are close to gravitational virial equilibrium, with $M/M_{\rm vir} \gtrsim$ 0.3–0.5, and will form stars in the near future. These prestellar condensations generally have flat inner density profiles, like isolated prestellar cores, but are distinguished by compact, finite sizes of a few thousand AU. The typical fragmentation lengthscale derived from the average projected separation between condensations is $\sim$6000 AU in $\rho$ Oph. This is $\sim$5 times smaller than the radial extent of isolated dense cores in the Taurus cloud (see Gómez et al. 1993).

Figure 5 shows the mass distribution of the 59 $\rho$ Oph prestellar fragments. It follows approximately $\Delta N/\Delta M \propto M^{-1.5}$ below $\sim$0.5 $M_\odot$, which is similar to the clump mass spectrum found by large-scale molecular line studies (e.g., Blitz 1993 and the chapter by Williams et al., this volume). The novel feature, however, is that the fragment mass spectrum found at 1.3 mm in $\rho$ Oph appears to steepen to $\Delta N/\Delta M \propto M^{-2.5}$ above $\sim$0.5 $M_\odot$. A similarly steep mass spectrum above $\sim$0.5 $M_\odot$ was obtained by Testi and Sargent (1998) for compact 3-mm starless condensations in the Serpens core. These prestellar mass spectra resemble the shape of the *stellar* initial mass function (IMF), which is known to approach $\Delta N/\Delta M_\star \propto M_\star^{-2.7}$ for 1 $M_\odot \lesssim M_\star \lesssim$ 10 $M_\odot$ and $\Delta N/\Delta M_\star \propto M_\star^{-1.2}$ for 0.1 $M_\odot \lesssim M_\star \lesssim$ 1 $M_\odot$ (e.g., Kroupa et al. 1993; Tinney 1993, 1995; Scalo 1998; see also the chapter by Meyer et al., this volume). Given the factor of $\sim$2 uncertainty on the measured prestellar masses, such a resemblance is remarkable and

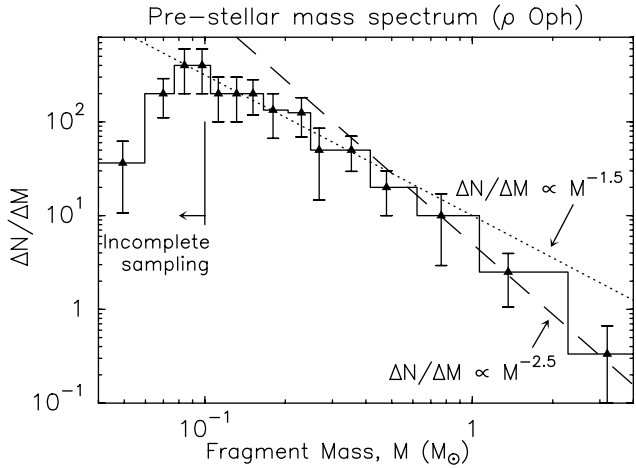


Figure 5. Mass spectrum of the 59 prestellar fragments extracted from the $\rho$ Oph 1.3 mm continuum mosaic shown in Color Plate 3 (from Motte et al. 1998). For comparison, dotted and long-dashed lines show power laws of the form $\Delta N/\Delta M \propto M^{-1.5}$ and $\Delta N/\Delta M \propto M^{-2.5}$, respectively. This prestellar mass spectrum is remarkable in that it resembles the shape of the IMF.

suggests that the IMF of embedded clusters is primarily determined at the prestellar stage of star formation (see also section IV below).

## III. THE YOUNGEST PROTOSTARS

### A. Class 0 Protostars and Other YSO Stages

*1. Infrared YSO Classes.* In the near/mid-infrared, three broad classes of YSOs can be distinguished based on the slopes of their SEDs between 2.2 $\mu$m and 10–25 $\mu$m, $\alpha_{\rm IR} = d\ \log(\lambda F_\lambda)/d\ \log(\lambda)$, which are interpreted in terms of an evolutionary sequence (Lada and Wilking 1984; Lada 1987). Going backward in time, Class III ($\alpha_{\rm IR} < -1.5$) and Class II ($-1.5 < \alpha_{\rm IR} < 0$) sources correspond to pre-main-sequence (PMS) stars ("weak" and "classical" T Tauri stars, respectively), surrounded by a circumstellar disk (optically thin in Class III and optically thick in Class II at $\lambda \lesssim 10\ \mu$m), but lacking a dense circumstellar envelope (see André and Montmerle 1994). The youngest YSOs detected at 2 $\mu$m are the Class I sources, which are characterized by $\alpha_{\rm IR} > 0$ (e.g., Wilking et al. 1989) and the close association with dense molecular gas (e.g., Myers et al. 1987). Class I objects are now interpreted as relatively evolved protostars with typical ages $\sim$1–2 $\times\ 10^5$ yr (e.g., Barsony and Kenyon 1992; Greene et al. 1994; Kenyon and Hartmann 1995), surrounded by both a disk and a diffuse circumstellar envelope of substellar ($\lesssim$0.1–0.3 $M_\odot$) mass (Whitney and Hartmann 1993; Kenyon et al. 1993*b*; André and Montmerle 1994; Lucas and Roche 1997). Their SEDs are successfully modeled in the framework of the "standard" theory of isolated protostars (e.g., Adams et al. 1987; Kenyon et al. 1993*a*), in agreement with the idea that they derive a substantial fraction of their luminosity from accretion (see also Greene and Lada 1996 and Kenyon et al. 1998).

*2. Class 0 Protostars.* Several condensations detected in submillimeter dust continuum maps of molecular clouds (such as those described in section II.E) appear to be associated with formed, hydrostatic YSOs and have been designated "Class 0" protostars (André et al. 1993). Specifically, Class 0 objects are defined by the following observational properties (André et al. 1993):

(i) Indirect evidence for a central YSO, as indicated by, e.g., the detection of a compact centimeter radio continuum source, a collimated CO outflow, or an internal heating source.
(ii) Centrally peaked but extended submillimeter continuum emission tracing the presence of a spheroidal circumstellar dust envelope (as opposed to just a disk).
(iii) High ratio of submillimeter to bolometric luminosity, suggesting that the envelope mass exceeds the central stellar mass: $L_{\rm smm}/L_{\rm bol} > 0.5\%$, where $L_{\rm smm}$ is measured longward of 350 $\mu$m. In practice, this often means an SED resembling a single-temperature blackbody at $T \sim$ 15–30 K (see Fig. 2).

Property (i) distinguishes Class 0 objects from the prestellar cores and condensations discussed in section II. In particular, deep VLA observations reveal no compact radio continuum sources in the centers of prestellar cores (Bontemps 1996; Yun et al. 1996). Properties (ii) and (iii) distinguish Class 0 objects from more evolved (Class I and Class II) YSOs. As shown by André et al. (1993), the $L_{\rm smm}/L_{\rm bol}$ ratio should roughly track the ratio $M_{\rm env}/M_\star$ of envelope to stellar mass and may be used as an evolutionary indicator (decreasing with time) for low-luminosity ($L_{\rm bol} \lesssim 50\,{\rm L}_\odot$) embedded YSOs. Criterion (iii) approximately selects objects that have $M_{\rm env}/M_\star > 1$, assuming plausible relations between $L_{\rm bol}$ and $M_\star$ on the one hand and between $L_{\rm smm}$ and $M_{\rm env}$ on the other (see André et al. 1993; André and Montmerle 1994). [A roughly equivalent criterion is $M_{\rm env}/L_{\rm bol} > 0.1\ {\rm M}_\odot/{\rm L}_\odot$.] Class 0 objects are therefore excellent candidates for being very young accreting protostars in which a hydrostatic core has formed but not yet accumulated the majority of its final mass. In practice, most of the confirmed Class 0 objects listed in Table I have $L_{\rm smm}/L_{\rm bol} \gg 0.5\%$ and are likely to be at the beginning of the main accretion phase with $M_{\rm env} \gg M_\star$ (see Fig. 6b).

*3. Evolutionary Diagrams for Embedded YSOs.* Combining infrared and submillimeter data, it is therefore possible to define a complete, empirical evolutionary sequence (Class 0 → Class I → Class II → Class III) for low-mass YSOs, which likely correspond to conceptually different stages of evolution: (early) main accretion phase, late accretion phase, PMS stars with protoplanetary disks, PMS stars with debris disks (see André and Montmerle 1994). This sequence is quasicontinuous and may be parameterized by the "bolometric temperature," $T_{\rm bol}$, defined by Myers and Ladd (1993) as the temperature of a blackbody having the same mean frequency as the observed YSO SED. Myers and Ladd proposed to use the $L_{\rm bol}$–$T_{\rm bol}$ diagram for embedded YSOs as a direct analog to the HR diagram for optically visible stars. As shown by Chen et al. (1995, 1997), YSOs with known classes have distinct ranges of $T_{\rm bol}$: <70 K for Class 0, 70–650 K for Class I, 650–2880 K for Class II, and >2880 K for Class III (e.g., Fig. 6a). The evolution of $T_{\rm bol}$ and $L_{\rm bol}$ from the Class 0 stage to the zero-age main sequence (ZAMS) has been modeled in the context of various envelope dissipation scenarios by Myers et al. (1998).

A perhaps more direct approach to tracking the circumstellar evolution of YSOs is to use the circumstellar mass $M_{c\star}$ derived from (sub)-millimeter continuum measurements of optically thin dust emission. Such measurements show that $M_{c\star}$ ($= M_{\rm env} + M_{\rm disk}$) is generally dominated by $M_{\rm env}$ in Class 0/Class I sources (e.g., Terebey et al. 1993) and decreases by a factor ~5–10 on average from one YSO class to the next (André and Montmerle 1994). In the spirit of the $L_{\rm smm}/L_{\rm bol}$ evolutionary indicator of André et al. (1993), Saraceno et al. (1996*a*) proposed the $L_{\rm smm}$–$L_{\rm bol}$ (or equivalently $M_{\rm env}$–$L_{\rm bol}$) diagram as an alternative evolutionary diagram for self-embedded YSOs. While $L_{\rm smm}$ and $M_{\rm env}$ are well correlated with $L_{\rm bol}$ for the majority of embedded YSOs (e.g., Reipurth et al. 1993),

**TABLE I**

Properties of Confirmed Class 0 Protostars

| Object | $\alpha$(2000) | $\delta$(2000) | Dist. (pc) | $L_{bol}$ ($L_\odot$) | $M_{env}$ ($M_\odot$) | $L_{smm}/L_{bol}$ (%)[a] | $T_{bol}$ (K) | Outflow Manifestations | Infall | Structure[b] | References[c] |
|---|---|---|---|---|---|---|---|---|---|---|---|
| W3OH-TW[d] | 02:27:04.7 | +61:52:24 | 2200 | $10^3$–$10^4$ | ~20 | ~1 | ≳80? | $H_2O$, radio | — | — | 1 |
| L1448-IRS2 | 03:25:22.4 | +30:45:12 | 300 | 6 | 0.9 | 3 | 70? | CO | — | — | 2 |
| L1448-N | 03:25:36.3 | +30:45:15 | 300 | 11 | 2.3 | 3 | 70 | CO, radio | Y? | D, B | 3,4,5,6,7,8,9,10 |
| L1448-C | 03:25:38.8 | +30:44:05 | 300 | 9 | 1.4 | 2 | 60 | CO, radio, $H_2$ | N? | D | 3,4,5,11,12,8,10,13 |
| NGC1333-IRAS2 | 03:28:55.4 | +31:14:35 | 350 | 40 | 1.7 | ≲1 | 50 | CO, $H_2$ | Y? | — | 14,15,9,16,17,13 |
| SVS13B | 03:29:03.1 | +31:15:52 | 350 | ~7 | 2.7 | ~5 | ~30 | SiO, $H_2$ | — | — | 18,19,20,21,22 |
| NGC1333-IRAS4A | 03:29:10.3 | +31:13:31 | 350 | 14 | 7. | 5 | 34 | CO, radio | Y | D, B | 23,24,15,16,25,26,27,28,10,13 |
| NGC1333-IRAS4B | 03:29:12.0 | +31:13:09 | 350 | 14 | 2.7 | 3 | 36 | CO, radio | Y | D, B | 23,24,15,16,25,28,10,13 |
| IRAS 03282 | 03:31:20.8 | +30:45:31 | 300 | 1.5 | 0.6 | 5 | 35 | CO, $H_2$ | — | — | 29,30,8 |
| HH211-MM | 03:43:56.8 | +32:00:50 | 300 | 5 | 1.5 | ~4 | ~30 | $H_2$ | — | — | 31,32 |
| IRAM 04191 | 04:21:56.9 | +15:29:46 | 140 | 0.15 | 0.5 | 12 | 18 | CO, radio | Y | N? | 33 |
| L1527[e] | 04:39:53.9 | +26:03:10 | 140 | 2 | 0.4 | 0.7 | 60 | CO, $H_2$ | Y | D | 34,35,36,37,38,6,10,13 |
| HH114MMS | 05:18:15.2 | +07:12:03 | 450 | ≲25 | 2.8 | ≳1 | ~40 | Radio, HH | — | — | 19 |
| RNO43-MM | 05:32:19.4 | +12:49:42 | 400 | 5 | 0.6 | ~5 | 36 | CO, radio, $H_2$ | N? | — | 39,19,40,41,10 |
| OMC3-MM6 | 05:35:23.5 | −05:01:32 | 450 | <60 | 12 | ≳2 | ~30 | CO, $H_2$ | — | — | 42,43 |
| L1641-VLA1[e] | 05:36:22.8 | −06:46:07 | 450 | 50 | 6.5 | ~3 | 70? | Radio, HH | — | — | 44,19,45 |
| NGC2023-MM1 | 05:41:24.8 | −02:18:09 | 450 | ~8 | 1.8–4.6 | ~3–10 | ~30 | CO | — | — | 46,47 |
| NGC2024-FIR5 | 05:41:44.5 | −01:55:43 | 450 | ≳10 | 15. | ≲30 | 20 | CO | N? | D, B? | 48,49,50,10 |
| NGC2024-FIR6 | 05:41:45.2 | −01:56:05 | 450 | ≳15 | 6. | ≲10 | 20 | CO | N? | — | 48,49,50,10 |

**TABLE I (CONT'D)**

| Object | $\alpha$(2000) | $\delta$(2000) | Dist. (pc) | $L_{bol}$ ($L_\odot$) | $M_{env}$ ($M_\odot$) | $L_{smm}/L_{bol}$ (%)[a] | $T_{bol}$ (K) | Outflow Manifestations | Infall | Structure[b] | References[c] |
|---|---|---|---|---|---|---|---|---|---|---|---|
| HH212-MM | 05:43:51.5 | −01:02:52 | 400 | 14 | 1.2 | ∼2 | 70? | CO, $H_2$ | — | — | 39,19,51 |
| HH24MMS | 05:46:08.3 | −00:10:42 | 450 | 5 | 4 | 10 | 20? | Radio, $H_2$ | — | D | 52,53,54,55,9,56 |
| HH25MMS[e] | 05:46:07.5 | −00:13:36 | 450 | 6 | 0.5 | 5 | 34 | CO, radio, $H_2$ | Y? | — | 54,57,10 |
| NGC2264G-VLA2 | 06:41:11.1 | +09:55:59 | 800 | 12 | 2 | 2 | 25 | CO, radio | — | — | 58,59,60 |
| IRAS 08076[e] | 08:09:32.8 | −36:05:00 | 400 | 17 | 2.3 | ≳1 | 74 | CO, $H_2$ | — | — | 61,16,62 |
| BHR71-MM | 12:01:36.3 | −65:08:44 | 200 | 10 | 2.4 | ∼3 | 56 | CO, HH | — | — | 63,62 |
| IRAS 13036[e] | 13:07:36.1 | −77:00:05 | 200 | 1.7 | 0.3 | ≲2 | 60 | CO | Y | — | 62,64,13 |
| VLA 1623 | 16:26:26.4 | −24:24:30 | 160 | 1 | 0.7 | 10 | <35 | CO, radio, $H_2$ | Y? | D, B? | 65,66,67,68,69,70,9,10,13,71,22 |
| IRAS 16293 | 16:32:22.7 | −24:28:32 | 160 | 23 | 2.3 | 2 | 43 | CO, radio | Y | D, B | 72,73,74,75,26,27,76,77,10,13 |
| Trifid-TC3[d] | 18:02:07.0 | −23:05:11 | 1680 | $\sim 10^3$ | ∼60 | ∼1 | ∼30 | SiO | — | — | 78 |
| L483-MM[e] | 18:17:29.8 | −04:39:38 | 200 | 9 | 0.3 | ∼0.7 | 50 | CO, radio | Y? | — | 79,37,10,13 |
| Serp-S68N | 18:29:47.9 | +01:16:46 | 310 | 6 | 1.0 | 3 | 40? | CO, CS | Y? | — | 80,81,82,83,84,13 |
| Serp-FIRS1[e] | 18:29:49.9 | +01:15:20 | 310 | 46 | 3 | ∼1 | 51 | CO, radio, $H_2O$ | N? | N? | 85,80,81,82,86,87,84,10,13,88 |
| Serp-SMM4 | 18:29:57.1 | +01:13:15 | 310 | 9 | 3 | ∼3 | 35 | CO, radio | Y | N? | 85,81,82,84,89,10,13,88 |
| Serp-SMM3[e] | 18:29:59.7 | +01:14:00 | 310 | 8 | 0.9 | ∼1 | 40 | CO, $H_2$ | N? | N? | 85,81,82,84,90,10,88 |
| G34.24+0.13MM[d] | 18:53:21.5 | +01:13:45 | 3700 | 4000 | 100 | ∼0.5 | 50 | $CH_3OH$ | — | — | 91 |
| L723-MM | 19:17:53.7 | +19:12:20 | 300 | 3 | 0.6 | ∼4 | 50 | CO, radio | N? | — | 92,93,32,19,94,95,10 |
| B335 | 19:37:00.8 | +07:34:11 | 250 | 3 | 0.8 | 6 | 37 | CO, radio | Y | D? | 92,96,97,40,98,10,13,99 |

**TABLE I (CONT'D)**

| Object | $\alpha$(2000) | $\delta$(2000) | Dist. (pc) | $L_{bol}$ ($L_\odot$) | $M_{env}$ ($M_\odot$) | $L_{smm}/L_{bol}$ (%)[a] | $T_{bol}$ (K) | Outflow Manifestations | Infall | Structure[b] | References[c] |
|---|---|---|---|---|---|---|---|---|---|---|---|
| S106-SMM | 20:27:25.3 | +37:22:46 | 600 | $\gtrsim$24 | $\lesssim$10 | $\lesssim$8 | $\gtrsim$20 | Bip. H II, $H_2O$ | — | — | 100,70 |
| L1157-MM | 20:39:06.2 | +68:02:22 | 440 | 11 | 0.5 | ~5 | ~60 | CO, $H_2$ | Y | D? | 101,32,102,69,10,13 |
| GF9–2 | 20:51:30.1 | +60:18:39 | 200 | 0.3 | ~0.5 | ~10 | $\lesssim$20 | — | Y | — | 103,104,105 |
| CepE-MM | 23:03:13.1 | +61:42:26 | 730 | 75 | 7 | ~2 | ~60 | CO, $H_2$ | — | — | 106,107 |
| IRAS 23385[d] | 23:40:54.5 | +61:10:28 | 4900 | 16000 | 370 | ~0.7 | $\gtrsim$40 | SiO | — | — | 108 |

[a] $L_{smm}$ is the luminosity radiated longward of 350 $\mu$m; Class 0s are defined by $L_{smm}/L_{bol} > 0.5\%$ (see section III.A).

[b] Small-scale structure: D = presence of disk-like component; B = binary or multiple system; N = single object with no disk.

[c] References: (1) Wilner et al. 1995; (2) O'Linger et al. 1999; (3) Bachiller et al. 1990; (4) Curiel et al. 1990; (5) Bachiller et al. 1995; (6) Terebey et al. 1993; (7) Terebey and Padgett 1997; (8) Barsony et al. 1998; (9) Greaves et al. 1997; (10) Gregersen et al. 1997; (11) Bachiller et al. 1991*a*; (12) Bally et al. 1993; (13) Mardones et al. 1997; (14) Sandell et al. 1994; (15) Langer et al. 1996; (16) Hodapp and Ladd 1995; (17) Ward-Thompson et al. 1996; (18) Grossman et al. 1987; (19) Chini et al. 1997*a*; (20) Bachiller et al. 1998; (21) Lefloch et al. 1998; (22) Looney et al. 1999; (23) Sandell et al. 1991; (24) Blake et al. 1995; (25) Mundy et al. 1993; (26) Akeson and Carlstrom 1997; (27) Greaves and Holland 1998; (28) Lay et al. 1995; (29) Bachiller et al. 1991*b*; (30) Bachiller et al. 1994; (31) McCaughrean et al. 1994; (32) Motte 1998; (33) André et al. 1999; (34) Ladd et al. 1991; (35) Eiroa et al. 1994; (36) Bontemps et al. 1996*a*; (37) Myers et al. 1995; (38) Ohashi et al. 1997; (39) Zinnecker et al. 1992; (40) Anglada et al. 1992; (41) Bence et al. 1996; (42) Chini et al. 1997*b*; (43) Yu et al. 1997; (44) Pravdo et al. 1985; (45) Zavagno et al. 1997; (46) Sandell et al. 1999; (47) Launhardt et al. 1996; (48) Mezger et al. 1992; (49) Richer et al. 1992; (50) Wiesemeyer et al. 1997; (51) Zinnecker et al. 1998; (52) Chini et al. 1993; (53) Ward-Thompson et al. 1995*a*; (54) Bontemps et al. 1995; (55) Bontemps et al. 1996*b*; (56) Chandler et al. 1995; (57) Gibb and Davis 1998; (58) Gómez et al. 1994; (59) Ward-Thompson et al. 1995*b*; (60) Lada and Fich 1996; (61) Persi et al. 1994; (62) Henning and Launhardt 1998; (63) Bourke et al. 1997; (64) Lehtinen 1997; (65) André et al. 1990; (66) André et al. 1993; (67) Leous et al. 1991; (68) Dent et al. 1995; (69) Davis and Eislöffel 1995; (70) Holland et al. 1996; (71) Pudritz et al. 1996; (72) Walker et al. 1986; (73) Wootten 1989; (74) Mizuno et al. 1990; (75) Tamura et al. 1993; (76) Mundy et al. 1992; (77) Walker et al. 1994; (78) Cernicharo et al. 1998; (79) Fuller et al. 1995*a*; (80) McMullin et al. 1994; (81) Hurt and Barsony 1996; (82) White et al. 1995; (83) Wolf-Chase et al. 1998; (84) Hurt et al. 1996; (85) Casali et al. 1993; (86) Curiel et al. 1993; (87) Jenness et al. 1995; (88) Hogerheijde et al. 1999; (89) Bontemps 1996; (90) Herbst et al. 1997; (91) Hunter et al. 1998; (92) Davidson 1987; (93) Cabrit and André 1991; (94) Anglada et al. 1991; (95) Avery et al. 1990; (96) Chandler et al. 1990; (97) Cabrit et al. 1988; (98) Zhou et al. 1993; (99) Hirano et al. 1992; (100) Richer et al. 1993; (101) Umemoto et al. 1992; (102) Gueth et al. 1997; (103) Güsten 1994; (104) Wiesemeyer 1997; (105) Wiesemeyer et al. 1998; (106) Lefloch et al. 1996; (107) Ladd and Hodapp 1997; (108) Molinari et al. 1998.

[d] Candidate massive Class 0 object.

[e] Borderline Class 0.

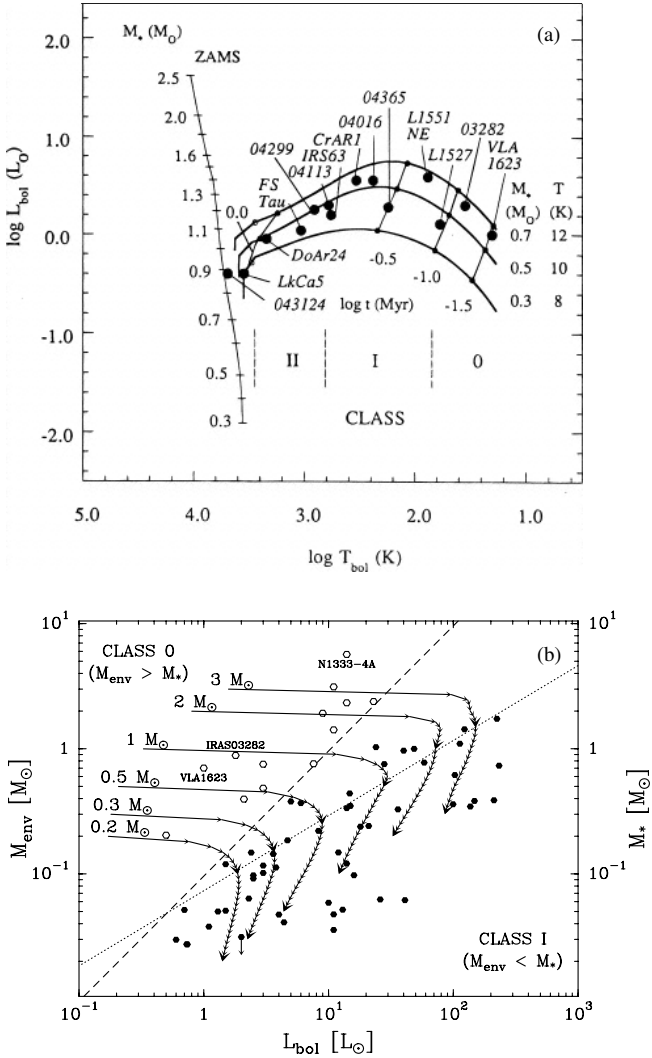


Figure 6. (a) $L_{\rm bol}$–$T_{\rm bol}$ diagram for 14 well-documented YSOs along with three model evolutionary tracks for various (final) stellar masses and cloud temperatures (from Myers et al. 1998). Four times, $t$(Myr), since the start of infall are indicated, at $\log t = -1.5$, $-1.0$, $-0.5$, and 0.0. (b) $M_{\rm env}$–$L_{\rm bol}$ diagram for a sample of Class I (filled circles) and confirmed Class 0 sources (open circles) mainly in Ophiuchus, Perseus, and Orion (adapted from André and Montmerle 1994 and Saraceno et al. 1996*a*). Evolutionary tracks shown are computed assuming that protostars form from bounded condensations of finite initial masses and have $L_{\rm bol} = GM_\star \dot{M}_{\rm acc}/R_\star + L_\star$, where $L_\star$ is the PMS birthline luminosity (e.g., Stahler 1988). $M_{\rm env}$ and $\dot{M}_{\rm acc} = M_{\rm env}/\tau$ (where $\tau = 10^5$ yr) have been assumed to decline exponentially with time (see Bontemps et al. 1996*a*). Small arrows are plotted on the tracks every $10^4$ yr, big arrows when 50% and 90% of the initial condensation has been accreted. The dashed and dotted lines are two $M_\star$–$L_{\rm bol}$ relations marking the conceptual border zone between the Class 0 ($M_{\rm env} > M_\star$) and Class I ($M_{\rm env} < M_\star$) stages; the dashed line has $M_\star \propto L_{\rm bol}$ (cf. André et al. 1993; André and Montmerle 1994), while the dotted line has $M_\star \propto L_{\rm bol}^{0.6}$, as suggested by the accretion scenario adopted in the tracks.

Class 0 objects clearly stand out from Class I sources in this diagram as objects with excess (sub)millimeter emission, that is, excess circumstellar material (see Fig. 6b). Moreover, one may compare the locations of observed embedded sources in the $M_{\rm env}$–$L_{\rm bol}$ diagram with simple protostellar evolutionary tracks (Saraceno et al. 1996*a*,*b*). Qualitatively at least, scenarios in which the mass accretion rate decreases with time for a given protostar (Bontemps et al. 1996a; Myers et al. 1998; see also section III.D below) and increases with the mass of the initial precollapse fragment (e.g., Myers and Fuller 1993; Reipurth et al. 1993; Saraceno et al. 1996*b*) yield tracks in better agreement with observations than the constant-rate scenario discussed by Saraceno et al. (1996a). In particular, the peak accretion luminosity is reduced by a factor ~2–4 compared to the constant-rate scenario (cf. Bontemps et al. 1996*a*; Myers et al. 1998; Fig. 6b), which agrees better with observed luminosities (e.g., Kenyon and Hartmann 1995).

Inclination effects may *a priori* affect the positions of individual protostellar objects in these evolutionary diagrams. In particular, it has been claimed (e.g., Yorke et al. 1995; Sonnhalter et al. 1995; Men'shchikov and Henning 1997) that some Class I sources may potentially look like Class 0 objects when observed at high inclination angles to the line of sight. However, the fact that Class 0 objects are associated with outflows an order of magnitude more powerful than in Class I sources (see section III.D below) confirms that these two types of YSOs differ qualitatively from each other. Furthermore, some Class 0 sources are known to have small inclination angles (e.g., Cabrit and Bertout 1992; Greaves et al. 1997; Wolf-Chase et al. 1998). We also stress that existing (sub)millimeter maps of dust continuum and $C^{18}O$ emission provide direct evidence that both Class I and Class 0 objects are *self-embedded* in substantial amounts of circumstellar material distributed in spatially resolved, spheroidal envelopes (e.g., André and Montmerle 1994; Chen et al. 1997; Ladd et al. 1998; Dent et al. 1998; see also section III.B below). This material has the ability to absorb the optical and near IR emission from the underlying star-disk system and to reradiate it quasi-isotropically at longer far-IR and (sub)millimeter wavelengths. In such a self-embedded configuration, viewing angle effects are minimized, as confirmed by radiative transfer calculations (e.g., Efstathiou and Rowan-Robinson 1991; Yorke et al. 1995). Physically, this is because the bulk of the luminosity emerges at long wavelengths, where the envelope is effectively optically thin. However, the short-wavelength emission from the inner star-disk remains very dependent on viewing angle, implying that $T_{\rm bol}$ estimates should be somewhat more sensitive to orientation effects than $L_{\rm bol}$ and $L_{\rm smm}/L_{\rm bol}$.

*4. Protostar Surveys and Lifetime Estimates.* Based on the key attributes of Class 0 protostars (see section III.A.2 above), various strategies can be used to search for and discover new candidates: (sub)millimeter continuum mapping (e.g., Mezger et al. 1992; Casali et al. 1993; Sandell and Weintraub 1994; Reipurth et al. 1996; Launhardt et al. 1996; Chini

et al. 1997*a*, *b*; Motte et al. 1998; André et al. 1999), high-resolution (HIRES) processing of the IRAS data (Hurt and Barsony 1996; O'Linger et al. 1999), deep radio continuum VLA surveys (e.g., Leous et al. 1991; Bontemps et al. 1995; Yun et al. 1996; Moreira et al. 1997; Gibb 1999), CO mapping (e.g., Bachiller et al. 1990; André et al. 1990; Bourke et al. 1997), and large-scale near IR/optical imaging of shocked $H_2$ and [S II] emission (e.g., Hodapp and Ladd 1995; Yu et al. 1997; Wilking et al. 1997; Gómez et al. 1998; Stanke et al. 1998; Phelps and Barsony 2000).

Class 0 objects appear to be short-lived compared to both prestellar cores/fragments (see section II above) and Class I near-IR sources. For example, in the $\rho$ Oph main cloud, where the mapping study of Motte et al. (1998) with the Institut de Radio Astronomie Millimétrique (IRAM) 30-m telescope provides a reasonably complete census of both pre- and protostellar condensations down to $\lesssim 0.1$ $M_\odot$, there are only two good Class 0 candidates (including the prototypical object VLA 1623; see André et al. 1993), whereas there are 15 to 30 near-IR Class I sources (e.g., Wilking et al. 1989; André and Montmerle 1994; Greene et al. 1994; Barsony and Ressler 2000; Bontemps et al. 1999).

Under the assumption that $\rho$ Oph is representative and forming stars at a roughly constant rate, the lifetime of Class 0 objects should thus be approximately an order of magnitude shorter than the lifetime of Class I sources (see Section III.A.1 above), i.e., typically $\sim 1$–$3 \times 10^4$ yr. The jetlike morphology and short dynamical timescales of Class 0 outflows are consistent with this estimate (e.g., Barsony et al. 1998; see section III.D below). A lifetime as short as a few $10^4$ yr supports the interpretation of Class 0 objects as very young accreting protostars (see, e.g., Fletcher and Stahler 1994 and Barsony 1994).

Regions such as the Serpens, Orion, and Perseus/NGC 1333 complexes seem to be particularly rich in Class 0 objects, and this is indicative of fairly high levels of ongoing, probably induced star formation activity (e.g., Hurt and Barsony 1996; Chini et al. 1997*b*; Yu et al. 1997; Barsony et al. 1998). For instance, we estimate the current star formation rate in Orion OMC-3 to be $\sim 2 \times 10^{-3}$ $M_\odot$ $yr^{-1}$, which is 1–2 orders of magnitude larger than the star formation rates characterizing the Trapezium, NGC 1333, and IC 348 near IR clusters when averaged over $\gtrsim 10^6$ yr periods (see Lada et al. 1996).

### B. Density Structure of the Protostellar Environment

*1. Envelope.* In contrast to prestellar cores, the envelopes of low-mass Class 0 and Class I *protostars* are always found to be strongly centrally condensed and do not exhibit any inner flattening in their (sub)millimeter continuum radial intensity profiles. In practice, this means that, when protostars are mapped with the resolution of the largest single-dish telescopes, the measured peak flux density is typically a fraction $\gtrsim$20% of the flux integrated over five beam widths. For comparison, the same fraction is

$\lesssim$10% for prestellar cores. (Sub)millimeter continuum maps indicate that protostellar envelopes in regions of isolated star formation such as Taurus have radial density gradients generally consistent with $\rho(r) \propto r^{-p}$, with $p \sim 1.5$–2, over more than ~10,000–15,000 AU in radius (e.g., Walker et al. 1990; Ladd et al. 1991; Motte 1998; Motte and André 1999; see also the chapter by Mundy et al., this volume). The estimated density gradient thus agrees with most collapse models, which predict a value of $p$ between 1.5 and 2 during the protostellar accretion phase (e.g., Whitworth and Summers 1985). Some studies have, however, inferred shallower density gradients ($p \sim 0.5$–1; e.g., Barsony and Chandler 1993; Chandler et al. 1998). In any case, the densities and masses measured for the envelopes around the bona fide Class I objects of Taurus appear to be consistent within a factor of ~4 with the predictions of the "standard" inside-out collapse theory (e.g., Shu et al. 1993) for $\sim 10^5$-yr-old, isolated protostars (Motte 1998; Motte and André 1999).

The situation is markedly different in star-forming clusters. In $\rho$ Ophiuchi in particular, the circumstellar envelopes of Class I and Class 0 protostars are observed to be very compact: they merge with dense cores, other envelopes, or the diffuse ambient cloud at a finite radius $R_{\rm out} \lesssim 5000$ AU (Motte et al. 1998). This is $\gtrsim$3 times smaller than the collapse expansion wavefront at a "Class I age" of $\sim 2 \times 10^5$ yr in the standard theory of isolated protostars, emphasizing the fact that each YSO has a finite "sphere of influence" in $\rho$ Oph. Similar results were obtained in the case of the Perseus Class 0 sources NGC 1333-4A, NGC 1333-2, L1448-C, and L1448-N (e.g., Motte 1998). Moreover, the envelopes of these Perseus protostars are 3 to 10 times denser than the singular isothermal sphere for a sound speed $a = 0.2$ km s$^{-1}$. This suggests that, prior to collapse, the main support against gravity was turbulent or magnetic in origin rather than purely thermal (see also Mardones et al. 1997).

*2. Disks and Multiplicity.* Many Class 0 protostars are seen to be multiple systems when viewed at subarcsecond resolution, sharing a common envelope and sometimes a circumbinary disk (e.g., Looney et al. 1999; see also col. 11 of Table I and the chapter by Mundy et al., this volume). These protobinaries probably formed by dynamical fragmentation during (or at the end of) the isothermal collapse phase (e.g., Chapman et al. 1992; Bonnell 1994; Boss and Myhill 1995). Interestingly enough, only cores with inner density profiles as flat as $\rho \propto r^{-1}$ or flatter (like observed prestellar cores; see section II), can apparently fragment during collapse (Myhill and Kaula 1992; Boss 1995; Burkert et al. 1997).

Despite the difficulty of discriminating between the disk and envelope components, existing (sub)millimeter continuum interferometric measurements suggest that the "disks" of Class 0 objects are a factor of $\gtrsim$10 less massive than their surrounding circumstellar envelopes (e.g., Chandler et al. 1995; Pudritz et al. 1996; Looney et al. 1999; Hogerheijde 1998; Motte 1998; and the chapter by Wilner and Lay, this volume).

### C. Direct Evidence for Infall

Rather convincing spectroscopic signatures of gravitational infall have been reported for several Class 0 objects, confirming their protostellar nature (e.g., Walker et al. 1986; Zhou et al. 1993; Gregersen et al. 1997; Mardones et al. 1997; see also col. 10 of Table I). Inward motions can be traced by optically thick molecular lines, which should (locally) exhibit asymmetric self-absorbed profiles skewed to the blue (see the chapter by Myers et al., this volume). The interpretation is often complicated by the simultaneous presence of rotation, outflow, or both (e.g., Menten et al. 1987; Walker et al. 1994; Cabrit et al. 1996).

A comprehensive survey of a sample of 47 embedded YSOs in $H_2CO$ ($2_{12}$–$1_{11}$) and CS (2–1) suggests that infall is more prominent in Class 0 than in Class I sources (Mardones et al. 1997). In these transitions, infall asymmetries are detected in 40–50% of Class 0 objects but less than 10% of Class I sources. This is qualitatively consistent with a decline of infall/accretion rate with evolutionary stage (see section III.D below). However, a more recent survey by Gregersen et al. (1999) using $HCO^+$ (3–2) finds no difference in the fraction of sources with "blue profiles" between Class 0 and Class I sources. The $HCO^+$ (3–2) line is more optically thick than $H_2CO$ ($2_{12}$–$1_{11}$) and CS (2–1), and is therefore a better tracer of infall at advanced stages. This result shows that some infall is still present at the Class I stage, but it remains consistent with a decline of the net accretion rate with time. The outflow is so broad in Class I sources that there often appears to be little transfer of mass to the inner ~2000 AU radius region around these objects (e.g., Fuller et al. 1995*b*; Cabrit et al. 1996; Brown and Chandler 1999).

### D. Decline of Outflow and Inflow with Time

*1. Evolution from Class 0 to Class I.* Most, if not all, Class 0 protostars drive powerful, "jetlike" CO molecular outflows (see, e.g., Bachiller 1996 and the chapter by Richer et al., this volume, for reviews). The mechanical luminosities of these outflows are often of the same order as the bolometric luminosities of the central sources (e.g., Curiel et al. 1990; André et al. 1993; Barsony et al. 1998). In contrast, while there is good evidence that some outflow activity exists throughout the accretion phase (e.g., Terebey et al. 1989; Parker et al. 1991; Bontemps et al. 1996*a*), the CO outflows from Class I sources tend to be much less powerful and less collimated than those from Class 0 objects.

In an effort to quantify the evolution of mass loss during the protostellar phase, Bontemps et al. (1996*a*) obtained and analyzed a homogeneous set of CO (2–1) outflow data around a large sample of low-luminosity ($L_{\rm bol} < 50\ L_\odot$), nearby ($d < 450$ pc) self-embedded YSOs. Their results show that Class 0 objects lie an order of magnitude above the well-known (e.g., Cabrit and Bertout 1992) correlation between outflow momentum flux ($F_{\rm CO}$) and bolometric luminosity ($L_{\rm bol}$) holding for Class I sources

(see the $F_{CO}$–$L_{bol}$ diagram shown in Fig. 5 of Bontemps et al. 1996*a*). Furthermore, they found that $F_{CO}$ was well correlated with $M_{env}$ in their *entire* sample (including both Class I and Class 0 sources). The same correlation was noted independently on other source samples by Moriarty-Schieven et al. (1994), Hogerheijde et al. (1998), and Henning and Launhardt (1998). As argued by Bontemps et al. (1996*a*), this new correlation is independent of the $F_{CO}$–$L_{bol}$ correlation and most likely results from a progressive decrease of outflow power with time during the accretion phase. This is illustrated in the normalized $F_{CO}c/L_{bol}$ versus $M_{env}/L_{bol}^{0.6}$ diagram of Fig. 7, which should be essentially free of any luminosity effect.

Since magnetocentrifugal accretion/ejection models of bipolar outflows (e.g., Shu et al. 1994; Ferreira and Pelletier 1995; Fiege and Henriksen 1996; Ouyed and Pudritz 1997) predict a direct proportionality

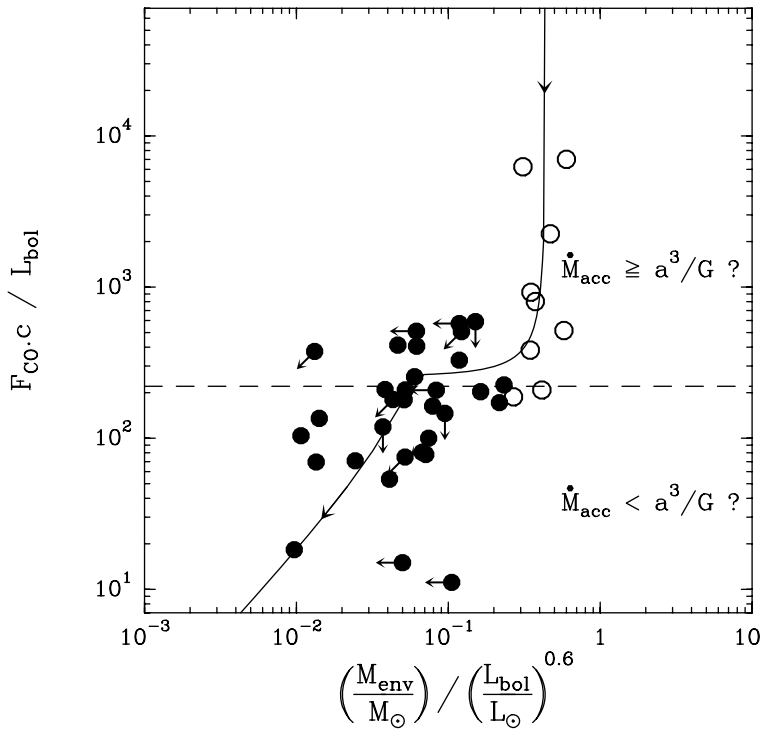


Figure 7. Normalized outflow momentum flux, $F_{CO}\ c/L_{bol}$, versus normalized envelope mass, $M_{env}/L_{bol}^{0.6}$, for a sample of Class 0 (open circles) and Class I (filled circles) objects (from Bontemps et al. 1996a). $F_{CO}\ c/L_{bol}$ can be taken as an empirical tracer of the accretion rate $\dot{M}_{acc}$, while $M_{env}/L_{bol}^{0.6}$ is an evolutionary indicator that decreases with time. This diagram should therefore mainly reflect the evolution of $\dot{M}_{acc}$ during the protostellar phase. The solid curve shows the accretion rate history predicted by the simplified collapse model of Henriksen et al. (1997).

between accretion and ejection, Bontemps et al. (1996*a*) proposed that the decline of outflow power with evolutionary stage seen in Fig. 7 reflects a corresponding decrease in the mass accretion rate. The results of Bontemps et al. (1996*a*) indicate that $\dot{M}_{\rm jet}$ declines from $\sim 10^{-6}$ $M_\odot$ yr$^{-1}$ for the youngest Class 0 protostars to $\sim 2 \times 10^{-8}$ $M_\odot$ yr$^{-1}$ for the most evolved Class I sources, suggesting a decrease in $\dot{M}_{\rm acc}$ from $\sim 10^{-5}$ $M_\odot$ yr$^{-1}$ to $\sim 2 \times 10^{-7}$ $M_\odot$ yr$^{-1}$ if realistic jet model parameters are adopted ($\dot{M}_{\rm jet}/\dot{M}_{\rm acc} \sim 0.1$–$0.3$, $V_{\rm jet} \sim 100$ km s$^{-1}$). These indirect estimates of $\dot{M}_{\rm acc}$ for Class 0 and Class I protostars should only be taken as indicative of the true evolutionary trend. Nevertheless, it is interesting to note that they agree well with independent estimates of the rates of envelope dissipation based on circumstellar mass versus age arguments (Ward-Thompson 1996; Ladd et al. 1998).

As illustrated by the evolutionary tracks of Fig. 6b, a decline of $\dot{M}_{\rm acc}$ with time does not imply a higher accretion luminosity for Class 0 objects compared to Class I sources, because the central stellar mass is smaller at the Class 0 stage and the stellar radius is likely to be larger (see Henriksen et al. 1997).

*2. Link with the Collapse Initial Conditions.* The apparent decay of $\dot{M}_{\rm acc}$ from the Class 0 to the Class I stage may be linked with the density structure observed for prestellar cores/condensations (Sect. II). (Magneto)hydrodynamic collapse models predict a time-dependent accretion history when the radial density profile at the onset of fast protostellar collapse differs from $\rho \propto r^{-2}$ (e.g., Foster and Chevalier 1993; Tomisaka 1996; McLaughlin and Pudritz 1997; Henriksen et al. 1997; Basu 1997; Safier et al. 1997; Li 1998; and Ciolek and Königl 1998). In particular, when starting from Bonnor-Ebert-like initial conditions resembling observed prestellar cores, these studies find that supersonic infall velocities develop prior to the formation of the central hydrostatic protostellar object at $t = 0$ (see, e.g., Foster and Chevalier 1993). Observationally, this early collapse phase should correspond to "isothermal protostars" (see section II.E for possible examples). During the protostellar accretion phase ($t > 0$), because of the significant infall velocities achieved at $t < 0$, $\dot{M}_{\rm acc}$ is initially higher than the standard $\sim a^3/G$ value obtained for the inside-out collapse of a static singular isothermal sphere (Shu 1977; see also section I). The accretion rate then converges toward the standard value of the Shu solution, and declines again below $a^3/G$ at late times if the reservoir of mass is finite. By comparison with the rough estimates of $\dot{M}_{\rm acc}$ given above, it is tempting to identify the short period of energetic accretion ($\dot{M}_{\rm acc} \sim 10 \times a^3/G$) predicted by the models just after point-mass formation with the observationally defined Class 0 stage (Henriksen et al. 1997; see Fig. 7). In this view, the more evolved Class I objects would correspond to the longer period of moderate accretion/ejection, when the accretion rate approaches the standard value ($\dot{M}_{\rm acc} \lesssim a^3/G \sim 2 \times 10^{-6}$ $M_\odot$ yr$^{-1}$ for a cloud temperature $\sim 10$ K).

Using simple pressure-free analytical calculations (justified, since the inflow becomes supersonic early on), Henriksen et al. (1997) could indeed find a good overall fit to the empirical accretion history inferred by Bontemps et al. (1996*a*) on the basis of CO outflow observations (see Fig. 7).

In the absence of magnetic fields, Foster and Chevalier (1993) showed that the timescale for convergence to the standard accretion rate of Shu (1977) depends on the radius of the flat inner core ($R_{\rm flat}$) relative to the outer radius of the initial precollapse condensation ($R_{\rm out}$). They found that a phase of constant $\sim a^3/G$ accretion rate is achieved only when $R_{\rm out}/R_{\rm flat} \gtrsim 20$, typically after $\sim$10 free-fall times of the flat inner region, for a period lasting $\sim$15 free-fall times when $R_{\rm out}/R_{\rm flat} = 20$ and progressively longer as $R_{\rm out}/R_{\rm flat}$ increases. Since observations suggest $R_{\rm out}/R_{\rm flat} \lesssim 3$ in Ophiuchus and $R_{\rm out}/R_{\rm flat} \gtrsim 15$ in Taurus (see sections II.C and III.B, and Motte et al. 1998), one may expect a marked time dependence of $\dot{M}_{\rm acc}$ in Ophiuchus but a reasonable agreement with the constant accretion rate of the self-similar theory of Shu et al. (1987, 1993) in Taurus. Indeed, Henriksen et al. (1997) note that there is a much better continuity between Class 0 and Class I protostars in Taurus than in Ophiuchus (see also André 1997).

Finally, we stress that the absolute values of $\dot{M}_{\rm acc}$ in the Class 0 and Class I stages are presently quite uncertain. An alternative interpretation of the evolution seen in Fig. 7 is that Class 0 protostars accrete at a rate roughly consistent with $\sim a^3/G$, while most Class I sources are in a terminal accretion phase with $\dot{M}_{\rm acc} \lesssim 0.1 \times a^3/G$, resulting from the finite effective reservoir of mass available to each object in clusters (e.g., Motte et al. 1998 and section III.B) or from the effects of outflows dispersing the envelope (e.g., Myers et al. 1998; Ladd et al. 1998). Distinguishing between this possibility and that advocated in the preceding paragraph will require direct measurements of the mass accretion rates.

## IV. CONCLUSIONS AND IMPLICATIONS

The observational studies discussed in section II demonstrate that prestellar cores and fragments are characterized by flat inner radial density gradients. This, in turn, suggests that the initial conditions for fast protostellar collapse are nonsingular; that is, the density profile at the onset of collapse is not infinitely centrally condensed. (Sub)millimeter observations also set strong constraints on protostellar evolution (section III). The fact that young (Class 0) protostars drive more powerful outflows than evolved (Class I) protostars suggests that the mass accretion rate $\dot{M}_{\rm acc}$ decreases by typically a factor of $\sim$5–10 from the Class 0 to the Class I stage (section III.D). Such a decline in $\dot{M}_{\rm acc}$ during the protostellar accretion phase may be the direct result of a flattened initial density profile (see section III.D). Based on these observational constraints, we suggest that most protostars form in a dynamical rather than quasistatic fashion.

The results summarized in this chapter also have broader implications concerning, e.g., the origin of the IMF. As pointed out in section II.E, the prestellar condensations observed in regions of multiple star formation such as $\rho$ Ophiuchi are finite-size structures, typically a few thousand AU in radius, which are clearly not scale-free. This favors a picture of star formation in clusters in which individual protostellar collapse is initiated in compact dense clumps, resulting from fragmentation and resembling finite-size Bonnor-Ebert cloudlets more than singular isothermal spheres. Such condensations may correspond to dense, low-ionization pockets decoupling themselves from the parent molecular cloud as a result of ambipolar diffusion or the dissipation of turbulence (e.g., Mouschovias 1991; Myers 1998; Nakano 1998). They would thus be free to undergo Jeans-like gravitational instabilities and collapse under the influence of external disturbances, of which there are many types in regions of multiple star formation (e.g., Pringle 1989; Whitworth et al. 1996; Motte et al. 1998; Barsony et al. 1998). By contrast, the low-density regions of the ambient cloud, being more ionized, would remain supported against collapse by static and turbulent magnetic fields. The typical separation between individual condensations should be of the order of the Jeans length in the parent cloud or core, in rough agreement with observations (e.g., Motte et al. 1998).

In this observationally driven scenario of fragmentation and collapse, stars are built from bounded fragments that represent finite reservoirs of mass. The star formation efficiency within these fragments is high: most of their "initial" masses at the onset of collapse end up in stars. If this is true, it implies that the physical mechanisms responsible for the formation of prestellar cores and condensations in molecular clouds, such as turbulent fragmentation (e.g., Padoan et al. 1997), play a key role in determining the IMF of embedded clusters. Such a picture, which we favor for regions of multiple star formation, is consistent with some theoretical scenarios of protocluster formation (e.g., Larson 1985; Klessen et al. 1998). It need not be universal, however, and it is in fact unlikely to apply to regions of isolated star formation such as the Taurus cloud. In these regions, protostars may accrete from larger reservoirs of mass, and feedback processes such as stellar winds may be more important in limiting accretion and defining stellar masses (e.g., Shu et al. 1987; Silk 1995; Adams and Fatuzzo 1996; Velusamy and Langer 1998).

With the advent of major new facilities at far-IR and (sub)millimeter wavelengths, the next decade promises to be at least as rich in observational discoveries as the past ten years. By combining the capabilities of a space telescope such as FIRST with those of a large ground-based interferometric array such as ALMA, it will be possible to study the detailed physics of complete samples of young protostars and precollapse fragments, in a variety of star-forming clouds, and down to the brown-dwarf mass regime. This should tremendously improve our global understanding of the initial stages of star formation in the Galaxy.

*Acknowledgments* We thank C. Correia for providing unpublished data shown in Fig. 2; G. Ciolek for Fig. 3b; P. Myers for Fig. 6a; and N. Grosso for assistance in preparing some of the figures. We are also grateful to F. Motte and the referee, N. Evans, for useful comments and suggestions.

## REFERENCES

Abergel, A., Bernard, J. P., Boulanger, F., et al. 1996. ISOCAM mapping of the $\rho$ Ophiuchi main cloud. *Astron. Astrophys.* 315:L329–L332.

Abergel, A., Bernard, J. P., Boulanger, F., et al. 1998. The dense core Oph D seen in extinction by ISOCAM. In *Star Formation with ISO,* ASP Conf. Ser. 132, ed. J. L. Yun and R. Liseau (San Francisco: Astronomical Society of the Pacific), pp. 220–229.

Adams, F. C., and Fatuzzo, M. 1996. A theory of the initial mass function for star formation in molecular clouds. *Astrophys. J.* 464:256–271.

Adams, F. C., Lada, C. J., and Shu, F. H. 1987. Spectral evolution of young stellar objects. *Astrophys. J.* 312:788–806.

Akeson, R. L., and Carlstrom, J. E. 1997. Magnetic field structure in protostellar envelopes. *Astrophys. J.* 491:254–266.

André, P. 1997. The evolution of flows and protostars. In *Herbig-Haro Flows and the Birth of Low Mass Stars,* IAU Symp. 182, ed. B. Reipurth and C. Bertout (Dordrecht: Kluwer), pp. 483–494.

André, P., and Montmerle, T. 1994. From T Tauri stars to protostars: Circumstellar material and young stellar objects in the $\rho$ Ophiuchi cloud. *Astrophys. J.* 420:837–862.

André, P., Martín-Pintado, J., Despois, D., and Montmerle, T. 1990. Discovery of a remarkable bipolar flow and exciting source in the $\rho$ Ophiuchi cloud core. *Astron. Astrophys.* 236:180–192.

André, P., Ward-Thompson, D., and Barsony, M. 1993. Submillimeter continuum observations of $\rho$ Ophiuchi A: The candidate protostar VLA 1623 and prestellar clumps. *Astrophys. J.* 406:122–141.

André, P., Ward-Thompson, D., and Motte, F. 1996. Probing the initial conditions of star formation: The structure of the prestellar core L1689B. *Astron. Astrophys.* 314:625–635.

André, P., Motte, F., and Bacmann, A. 1999. Discovery of an extremely young accreting protostar in Taurus. *Astrophys. J. Lett.,* 513:L57–L60.

Anglada, G., Estalella, R., Rodríguez, L. F., Torrelles, J. M., López, R., and Cantó, J. 1991. A double radio source at the center of the outflow in L723. *Astrophys. J.* 376:615–617.

Anglada, G., Rodríguez, L. F., Cantó, J., Estalella, R., and Torrelles, J. M. 1992. Radio continuum from the powering sources of the RNO 43, HARO 4-255 FIR, B335, and PV Cephei outflows and from the Herbig-Haro object 32A. *Astrophys. J.* 395:494–500.

Avery, L. W., Hayashi, S. S., and White, G. J. 1990. The unusual morphology of the high-velocity gas in L723: One outflow or two? *Astrophys. J.* 357:524–530.

Bachiller, R. 1996. Bipolar molecular outflows from young stars and protostars. *Ann. Rev. Astron. Astrophys.* 34:111–154.

Bachiller, R., Martín-Pintado, J., Tafalla, M., Cernicharo, J., and Lazareff, B. 1990. High-velocity molecular bullets in a fast bipolar outflow near L1448/IRS3. *Astron. Astrophys.* 231:174–186.

Bachiller, R., André, P., and Cabrit, S. 1991*a*. Detection of the exciting source of the spectacular molecular outflow L1448 at λλ 1–3 mm. *Astron. Astrophys.* 241:L43–L46.

Bachiller, R., Martín-Pintado, J., and Planesas, P. 1991*b*. High-velocity molecular jets and bullets from IRAS 03282+3035. *Astron. Astrophys.* 251:639–648.

Bachiller, R., Terebey, S., Jarrett, T., Martín-Pintado, J., Beichman, C. A., and van Buren, D. 1994. Shocked molecular gas around the extremely young source IRAS 03282+3035. *Astrophys. J.* 437:296–304.

Bachiller, R., Guilloteau, S., Dutrey, A., Planesas, P., and Martín-Pintado, J. 1995. The jet-driven molecular outflow in L 1448. CO and continuum synthesis images. *Astron. Astrophys.* 299:857–868.

Bachiller, R., Guilloteau, S., Gueth, F., Tafalla, M., Dutrey, A., Codella, C., and Catsets, A. 1998. A molecular jet from SVS 13B near HH 7-11. *Astron. Astrophys.* 339:L49–L52.

Bacmann, A., André, P., Abergel, A., et al. 1998. An ISOCAM absorption study of dense cloud cores. In *Star Formation with ISO,* ASP Conf. Ser. 132, ed. J. L. Yun and R. Liseau (San Francisco: Astronomical Society of the Pacific), pp. 307–313.

Bally, J., Lada, E. A., and Lane, A. P. 1993. The L1448 molecular jet. *Astrophys. J.* 418:322–327.

Balsara, D., Ward-Thompson, D., Pouquet, A., and Crutcher, R. M. 1998. An MHD model of the interstellar medium and a new method of accretion onto dense star-forming cores. In *Interstellar Turbulence,* ed. J. Franco and A. Carramiñana (Cambridge: Cambridge University Press), pp. 261–266.

Barsony, M. 1994. Class 0 protostars. In *Clouds, Cores, and Low-mass Stars,* ASP Conf. Ser. 65, ed. D. P. Clemens and R. Barvainis (San Francisco: Astronomical Society of the Pacific), pp. 197–206.

Barsony, M., and Chandler, C. J. 1993. The circumstellar density distribution of L1551NE. *Astrophys. J.* 406:L71–L74.

Barsony, M., and Kenyon, S. J. 1992. On the origin of submillimeter emission from young stars in Taurus-Auriga. *Astrophys. J.* 384:L53–L57.

Barsony, M., and Ressler, M. 2000. The initial luminosity function for L1688: New mid-IR imaging photometry. *Astrophys. J.,* in preparation.

Barsony, M., Ward-Thompson, D., André, P., and O'Linger, J. 1998. Protostars in Perseus: Outflow induced fragmentation. *Astrophys. J.* 509:733–748.

Basu, S. 1997. A semianalytic model for supercritical core collapse: Self-similar evolution and the approach to protostar formation. *Astrophys. J.* 485:240–253.

Basu, S., and Mouschovias, T. C. 1995. Magnetic braking, ambipolar diffusion, and the formation of cloud cores and protostars. III. Effect of the initial mass-to-flux ratio. *Astrophys. J.* 453:271–283.

Bate, M. R. 1998. Collapse of a molecular cloud core to stellar densities: The first three-dimensional calculations. *Astrophys. J. Lett.* 508:L95–L98.

Beckwith, S. V. W., Sargent A. I, Chini, R. S., and Guesten, R. 1990. A survey for circumstellar disks around young stellar objects. *Astron. J.* 99:924–945.

Beichman, C. A., Myers, P. C., Emerson, J. P., et al. 1986. Candidate solar-type protostars in nearby molecular cloud cores. *Astrophys. J.* 307:337–349.

Bence, S. J., Richer, J. S., and Padman, R. 1996. RNO 43: A jet-driven super-outflow. *Mon. Not. Roy. Astron. Soc.* 279:866–883.

Benson, P. J., and Myers, P. C. 1989. A survey for dense cores in dark clouds. *Astrophys. J. Sup.* 71:89–108.

Blake, G. A., Sandell, G., van Dishoeck, E. W., Groesbeck, T. D., Mundy, L. G., and Aspin, C. 1995. A molecular line study of NGC 1333/IRAS 4. *Astrophys. J.* 441:689–701.

Blitz, L. 1993. Giant molecular clouds. In *Protostars and Planets III,* ed. E. H. Levy and J. I. Lunine (Tucson: University of Arizona Press), pp. 125–161.

Blottiau, P., Chièze, J. P., and Bouquet, S. 1988. An asymptotic self-similar solution for the gravitational collapse. *Astron. Astrophys.* 207:24–36.

Bonnell, I. A. 1994. Fragmentation and the formation of binary and multiple systems. In *Clouds, Cores, and Low-mass Stars,* ASP Conf. Ser. 65, ed. D. P. Clemens and R. Barvainis (San Francisco: Astronomical Society of the Pacific), pp. 115–124.

Bonnell, I. A., Bate, M. R., Clarke, C. J., and Pringle, J. E. 1997. Accretion and the stellar mass spectrum in small clusters. *Mon. Not. Roy. Astron. Soc.* 285:201–208.

Bontemps, S. 1996. Evolution de l'éjection de matière des proto-étoiles. Ph.D. Dissertation, University of Paris, XI.

Bontemps, S., André, P., and Ward-Thompson, D. 1995. Deep VLA search for the youngest protostars: A Class 0 source in the HH24-26 region. *Astron. Astrophys.* 297:98–102.

Bontemps, S., André, P., Terebey, S., and Cabrit, S. 1996*a*. Evolution of outflow activity around low-mass embedded young stellar objects. *Astron. Astrophys.* 311:858–872.

Bontemps, S., Ward-Thompson, D., and André, P. 1996*b*. Discovery of a jet emanating from the protostar HH 24 MMS. *Astron. Astrophys.* 314:477–483.

Bontemps, S., Nordh, L., Olofsson, G., André, P., Huldtgren, M., Kaas, A. A., Abergel, A., Blommaert, J., Boulanger, F., Burgdorf, M., Cenarsky, C. J., Cenarsky, D., Copet, E., Davies, J., Falgarone, E., Lagouche, G., Montmerle, T., Pérault, M., Persi, P., Prunti, T., Puget, J. L., and Sibille, F. 1999. Constraints on the initial mass function from ISOCAM observations of the $\rho$ Ophiuchi embedded cluster. *Astron. Astrophys.*, submitted.

Boss, A. P. 1995. Gravitational collapse and binary protostars. *Rev. Mex. Astron. Astrofis. Ser. Conf.* 1:165–177.

Boss, A. P., and Myhill, E. A. 1995. Collapse and fragmentation of molecular cloud cores. III. Initial differential rotation. *Astrophys. J.* 451:218–224.

Boss, A. P., and Yorke, H. W. 1995. Spectral energy of first protostellar cores: Detecting "class −I" protostars with ISO and SIRTF. *Astrophys. J.* 439:L55–L58.

Bourke, T. L., Hyland, A. R., and Robinson, G. 1995*a*. Studies of star formation in isolated small dark clouds. I. A catalogue of southern Bok globules: Optical and IRAS properties. *Mon. Not. Roy. Astron. Soc.* 276:1052–1066.

Bourke, T. L., Hyland, A. R., Robinson, G., James, S. D., and Wright, C. M. 1995*b*. Studies of star formation in isolated small dark clouds. II. A southern ammonia survey. *Mon. Not. Roy. Astron. Soc.* 276:1067–1084.

Bourke, T. L., Garay, G., Lehtinen, K. K., et al. 1997. Discovery of a highly collimated molecular outflow in the southern Bok globule BHR 71. *Astrophys. J.* 476:781–800.

Brown, D. W., and Chandler, C. J. 1999. Circumstellar kinematics and the measurement of stellar mass for the protostars TMC1 and TMC1A. *Mon. Not. Roy. Astron. Soc.,* 303:855–863.

Burkert, A., Bate, M. R., and Bodenheimer, P. 1997. Protostellar fragmentation in a power-law density distribution. *Mon. Not. Roy. Astron. Soc.* 289:497–504.

Butner, H. M., Lada, E. A., and Loren, R. B. 1995. Physical properties of dense cores: DCO + observations. *Astrophys. J.* 448:207–225.

Cabrit, S., and André, P. 1991. An observational connection between circumstellar disk mass and molecular outflows. *Astrophys. J. Lett.* 379:L25–L28.

Cabrit, S., and Bertout, C. 1992. CO line formation in bipolar flows. III. The energetics of molecular flows and ionized winds. *Astron. Astrophys.* 261:274–284.

Cabrit, S., Goldsmith, P. F., and Snell, R. L. 1988. Identification of RNO 43 and B335 as two highly collimated bipolar flows oriented nearly in the plane of the sky. *Astrophys. J.* 334:196–208.

Cabrit, S., Guilloteau, S., André, P., Bertout, C., Montmerle, T., and Schuster, K. 1996. Plateau de Bure observations of HL Tauri: Outflow motions in a remnant circumstellar envelope. *Astron. Astrophys.* 305:527–540.

Casali, M. M., Eiroa, C., and Duncan, W. D. 1993. A second phase of star formation in the Serpens core. *Astron. Astrophys.* 275:195–200.

Ceccarelli, C., Caux, E., White, G. J., Molinari, S., Furniss, I., Liseau, R., and Nisini, B. 1998. The far infrared line spectrum of the protostar IRAS 16293-2422. *Astron. Astrophys.* 331:372–382.

Cernicharo, J., Lefloch, B., Cox, P., Cenarsky, D., Yusef-Zadeh, F., Mendez, D. I., Acosta-Pulido, J., López, R. J. G., and Heran, A. 1998. Induced massive star formation in the Trifid nebula? *Science* 282:462–465.

Chandler, C. J., Gear, W. K., Sandell, G., Hayashi, S., Duncan, W. D., and Griffin, M. J. 1990. B335: Protostar or embedded pre-main-sequence star? *Mon. Not. Roy. Astron. Soc.* 243:330–335.

Chandler, C. J., Koerner, D. W., Sargent, A. I., and Wood, D. O. S. 1995. Dust emission from protostars: The disk and envelope of HH 24 MMS. *Astrophys. J.* 449:L139–L142.

Chandler, C. J., Barsony, M., and Moore, T. J. T. 1998. The circumstellar envelopes around three protostars in Taurus. *Mon. Not. Roy. Astron. Soc.* 299:789–798.

Chapman, S. J., Davies, J. R., Disney, M. J., Nelson, A. H., Pongracic, H., Turner, J. A., Whitworth, A. P. 1992. The formation of binary and multiple star systems. *Nature* 359:207–210.

Chen, H., Myers, P. C., Ladd, E. F., and Wood, D. O. S. 1995. Bolometric temperature and young stars in the Taurus and Ophiuchus complexes. *Astrophys. J.* 445:377–392.

Chen, H., Grenfell, T. G., Myers, P. C., and Hughes, J. D. 1997. Comparison of star formation in five nearby molecular clouds. *Astrophys. J.* 478:295–312.

Chièze, J.-P., and Pineau des Forêts, G. 1987. The fragmentation of molecular clouds. II. Gravitational stability of low-mass molecular cloud cores. *Astron. Astrophys.* 183:98–108.

Chini, R., Krügel, E., Haslam, C. G. T., Kreysa, E., Lemke, R., Reipurth, B., Sievers, A., and Ward-Thompson, D. 1993. Discovery of a cold and gravitationally unstable cloud fragment. *Astron. Astrophys.* 272:L5–L8.

Chini, R., Reipurth, B., Sievers, A., Ward-Thompson, D., Haslam, C. G. T., Kreysa, E., and Lemke, R. 1997*a*. Cold dust around Herbig-Haro energy sources: Morphology and new protostellar candidates. *Astron. Astrophys.* 325:542–550.

Chini, R., Reipurth, B., Ward-Thompson, D., Bally, J., Nyman, L. A., Sievers, A., and Billawala, Y. 1997*b*. Dust filaments and star formation in OMC-2 and OMC-3. *Astrophys. J.* 474:L135–L138.

Ciolek, G. E., and Königl, A. 1998. Dynamical collapse of nonrotating magnetic molecular cloud cores: Evolution through point-mass formation. *Astrophys. J.* 504:257–279.

Ciolek, G. E., and Mouschovias, T. C. 1994. Ambipolar diffusion, interstellar dust, and the formation of cloud cores and protostars. III. Typical axisymmetric solutions. *Astrophys. J.* 425:142–160.

Clemens, D. P., and Barvainis, R. 1988. A catalog of small, optically selected molecular clouds: Optical, infrared, and millimeter properties. *Astrophys. J. Sup.* 68:257–286.

Curiel, S., Raymond, J. C., Rodríguez, L. F., Cantó, J., and Moran, J. M. 1990. The exciting source of the bipolar outflow in L1448. *Astrophys. J. Lett.* 365:L85–L88.

Curiel, S., Rodríguez, L. F., Moran, J. M., and Cantó, J. 1993. The triple radio continuum source in Serpens: The birth of a Herbig-Haro system? *Astrophys. J.* 415:191–203.

Davidson, J. A. 1987. Low-luminosity embedded sources and their environs. *Astrophys. J.* 315:602–620.

Davis, C. J., and Eislöffel, J. 1995. Near-infrared imaging in $H_2$ of molecular (CO) outflows from young stars. *Astron. Astrophys.* 300:851–869.

Dent, W. R. F., Matthews, H. E., and Walther, D. M. 1995. CO and shocked $H_2$ in the highly collimated outflow from VLA 1623. *Mon. Not. Roy. Astron. Soc.* 277:193–209.

Dent, W. R. F., Matthews, H. E., and Ward-Thompson, D. 1998. The submillimetre colour of young stellar objects. *Mon. Not. Roy. Astron. Soc.* 301:1049–1063.

Efstathiou, A., and Rowan-Robinson, M. 1991. Radiative transfer in axisymmetric dust clouds. II. Models of rotating protostars. *Mon. Not. Roy. Astron. Soc.* 252:528–534.

Eiroa, C., Miranda, L. F., Anglada, G., Estalella, R., and Torrelles, J. M. 1994. Herbig-Haro objects associated with extremely young sources in L1527 and L1448. *Astron. Astrophys.* 283:973–977.

Falgarone, E., and Puget, J.-L. 1985. A model of clumped molecular clouds. I. Hydrostatic structure of dense cores. *Astron. Astrophys.* 142:157–170.

Ferreira J., and Pelletier G. 1995. Magnetized accretion-ejection structures. III. Stellar and extragalactic jets as weakly dissipative disk outflows. *Astron. Astrophys.* 295:807–832.

Fiege, J. D., and Henriksen, R. N. 1996. A global model of protostellar bipolar outflow. I. *Mon. Not. Roy. Astron. Soc.* 281:1038–1054.

Fletcher, A. B., and Stahler, S. W. 1994. The luminosity functions of embedded stellar clusters. I: Method of solution and analytic results. *Astrophys. J.* 435:313–328.

Foster, P. N., and Chevalier, R. A. 1993. Gravitational collapse of an isothermal sphere. *Astrophys. J.* 416:303–311.

Fuller, G. A., Lada, E. A., Masson, C. R., and Myers, P. C. 1995*a*. The infrared nebula and outflow in Lynds 483. *Astrophys. J.* 453:754–760.

Fuller, G. A., Lada, E. A., Masson, C. R., and Myers, P. C. 1995*b*. The circumstellar molecular core around L1551 IRS 5. *Astrophys. J.* 454:862–871.

Gammie, C. F., and Ostriker, E. C. 1996. Can nonlinear hydromagnetic waves support a self-gravitating cloud? *Astrophys. J.* 466:814–830.

Gibb, A. G. 1999. A VLA search for embedded young stellar objects and protostellar candidates in L1630. *Mon. Not. Roy. Astron. Soc.,* 304:1–7.

Gibb, A. G., and Davis, C. J. 1998. The outflow from the class 0 protostar HH25MMS: Methanol enhancement in a well-collimated outflow. *Mon. Not. Roy. Astron. Soc.* 298:644–656.

Gómez, J. F., Curiel, S., Torrelles, J. M., Rodríguez, L. F., Anglada, G., and Girart, J. M. 1994. The molecular core and the powering source of the bipolar molecular outflow in NGC 2264G. *Astrophys. J.* 436:749–753.

Gómez, M., Hartmann, L., Kenyon, S. J., and Hewett, R. 1993. On the spatial distribution of pre-main-sequence stars in Taurus. *Astron. J.* 105:1927–1937.

Gómez, M., Whitney, B. A., and Wood, K. 1998. A survey of optical jets and Herbig-Haro objects in the $\rho$ Ophiuchi cloud core. *Astron. J.* 115:2018–2027.

Greaves, J. S., and Holland, W. S. 1998. Twisted magnetic field lines around protostars. *Astron. Astrophys.* 333:L23–L26.

Greaves, J. S., Holland, W. S., and Ward-Thompson, D. 1997. Submillimeter polarimetry of Class 0 protostars: Constraints on magnetized outflow models. *Astrophys. J.* 480:255–261.

Greene, T. P., and Lada, C. J. 1996. Near-infrared spectra and the evolutionary status of young stellar objects: Results of a 1.1–2.4 $\mu$m survey. *Astron. J.* 112:2184–2221.

Greene, T. P., Wilking, B. A., André, P., Young, E. T., and Lada, C. J. 1994. Further mid-infrared study of the $\rho$ Ophiuchi cloud young stellar population: Luminosities and masses of pre-main-sequence stars. *Astrophys. J.* 434:614–626.

Gregersen, E. M., Evans, N. J., II, Zhou, S., and Choi, M. 1997. New protostellar collapse candidates: An HCO+ survey of the Class 0 sources. *Astrophys. J.* 484:256–276.

Gregersen, E. M., Evans, N. J., II, Mardones, D., and Myers, P. C. 1999. Does infall end before the Class I stage? *Astrophys. J.,* in preparation.

Grossman, E. N., Masson, C. R., Sargent, A. I., Scoville, N. Z., Scott, S., and Woody, D. P. 1987. A possible protostar near HH 7-11. *Astrophys. J.* 320:356–363.

Gueth, F., Guilloteau, S., Dutrey, A., and Bachiller, R. 1997. Structure and kinematics of a protostar: mm-Interferometry of L 1157. *Astron. Astrophys.* 323:943–952.

Güsten, R. 1994. Protostellar condensations. In *The Cold Universe,* ed. T. Montmerle, C. J. Lada, I. F. Mirabel, and J. Trân Thanh Vân (Gif-sur-Yvette: Editions Frontières), pp. 169–177.

Henning, T., and Launhardt, R. 1998. Millimetre study of star formation in southern globules. *Astron. Astrophys.* 338:223–242.

Henning, T., Michel, B., and Stognienko, R. 1995. Dust opacities in dense regions. *Planet. Space Sci.* 43:1333–1343.

Henriksen, R. N., André, P., and Bontemps, S. 1997. Time-dependent accretion and ejection implied by prestellar density profiles. *Astron. Astrophys.* 323:549–565.

Herbst, T. M., Beckwith, S, and Robberto, M. 1997. A new molecular hydrogen outflow in Serpens. *Astrophys. J. Lett.* 486:L59–L62.

Hildebrand, R. H. 1983. The determination of cloud masses and dust characteristics from submillimetre thermal emission. *Quart. J. Roy. Astron. Soc.* 24:267–282.

Hirano, N., Kameya, O., Kasuga, T., and Umemoto, T. 1992. Bipolar outflow in B335. The small-scale structure. *Astrophys. J. Lett.* 390:L85–L88.

Hodapp, K.-W., and Ladd, E. F. 1995. Bipolar jets from extremely young stars observed in molecular hydrogen emission. *Astrophys. J.* 453:715–720.

Hogerheijde, M. R. 1998. The molecular environment of low-mass protostars. Ph.D. Dissertation, University of Leiden (Amsterdam: Thesis Publishers).

Hogerheijde, M. R., van Dishoeck, E. F., Blake, G. A., and van Langevelde, H. J. 1998. Envelope structure on 700 AU scales and the molecular outflows of low-mass young stellar objects. *Astrophys. J.* 502:315–336.

Hogerheijde, M. R., van Dishoeck, E. F., Salverda, J. M., and Blake, G. A. 1999. Envelope structure of deeply embedded young stellar objects in the Serpens molecular cloud. *Astrophys. J.,* 513:350–369.

Holland, W. S., Greaves, J. S., Ward-Thompson, D., and André, P. 1996. The magnetic field structure around protostars. Submillimetre polarimetry of VLA 1623 and S106-IR/FIR. *Astron. Astrophys.* 309:267–274.

Hunter, T. R., Neugebauer, G., Benford, D. J., Matthews, K., Lis, D. C., Serabyn, E., and Phillips, T. G. 1998. G34.24+0.13MM: A deeply embedded proto-B-star. *Astrophys. J. Lett.* 493:L97–L100.

Hurt, R. L., and Barsony, M. 1996. A cluster of Class 0 protostars in Serpens: An IRAS HIRES study. *Astrophys. J. Lett.* 460:L45–L48.

Hurt, R. L., Barsony, M., and Wootten, A. 1996. Potential protostars in cloud cores: $H_2CO$ observations of Serpens. *Astrophys. J.* 456:686–695.

Jenness, T., Scott, P. F., and Padman, R. 1995. Studies of embedded far-infrared sources in the vicinity of $H_2O$ masers-I. Observations. *Mon. Not. Roy. Astron. Soc.* 276:1024–1040.

Jessop, N., and Ward-Thompson, D. 1999. A far-infrared survey of molecular cloud cores. *Mon. Not. Roy. Astron. Soc.,* in press.

Johnstone, D., and Bally, J. 1999. JCMT/SCUBA sub-millimeter wavelength imaging of the integral-shaped filament in Orion. *Astrophys. J. Lett.* 510:L49–L53.

Kenyon, S. J., and Hartmann, L. 1995. Pre-main-sequence evolution in the Taurus-Auriga molecular cloud. *Astrophys. J. Suppl.* 101:117–171.

Kenyon, S. J., Calvet, N., and Hartmann, L. 1993*a*. The embedded young stars in the Taurus-Auriga molecular cloud. I. Models for spectral energy distributions. *Astrophys. J.* 414:676–694.

Kenyon, S. J., Whitney, B. A., Gomez, M., and Hartmann, L. 1993*b*. The embedded young stars in the Taurus-Auriga molecular cloud. II. Models for scattered light images. *Astrophys. J.* 414:773–792.

Kenyon, S. J., Brown, D. I., Tout, C. A., and Berlind, P. 1998. Optical spectroscopy of embedded young stars in the Taurus-Auriga molecular cloud. *Astron. J.* 115:2491–2591.

Klessen, R. S., Burkert, A., and Bate, M. R. 1998. Fragmentation of molecular clouds: The initial phase of a stellar cluster. *Astrophys. J. Lett.* 501:L205–L208.

Kroupa, P., Tout, C. A., and Gilmore, G. 1993. The distribution of low-mass stars in the Galactic disc. *Mon. Not. Roy. Astron. Soc.* 262:545–587.

Lada, C. J. 1987. Star formation: From OB associations to protostars. In *Star Forming Regions,* IAU Symp. 115, ed. M. Peimbert and J. Jugaku (Dordrecht: Reidel), pp. 1–18.

Lada, C. J., and Fich, M. 1996. The structure and energetics of a highly collimated bipolar outflow: NGC 2264G. *Astrophys. J.* 459:638–652.

Lada, C. J., and Wilking, B. 1984. The nature of the embedded population in the Rho Ophiuchi dark cloud. Mid-infrared observations. *Astrophys. J.* 287:610–621.

Lada, C. J., Alves, J., and Lada, E. A. 1996. Near-infrared imaging of embedded clusters: NGC 1333. *Astron. J.* 111:1964–1976.

Ladd, E. F., and Hodapp, K.-W. 1997. A double outflow from a deeply embedded source in Cepheus. *Astrophys. J.* 474:749–759.

Ladd, E. F., Adams, F. C., Casey, S., Davidson, J. A., Fuller, G. A., Harper, D. A., Myers, P. C., and Padman, R. 1991. Far-infrared and submillimeter wavelength observations of star-forming dense cores. II. Images. *Astrophys. J.* 382:555–569.

Ladd, E. F., Fuller, G. A., and Deane, J. R. 1998. $C^{18}O$ and $C^{17}O$ observations of embedded young stars in the Taurus molecular cloud. I. Integrated intensities and column densities. *Astrophys. J.* 495:871–890.

Langer, W. D., Castets, A., and Lefloch, B. 1996. The IRAS 2 and IRAS 4 outflows and star formation in NGC 1333. *Astrophys. J. Lett.* 471:L111–L114.

Larson, R. B. 1969. Numerical calculations of the dynamics of a collapsing protostar. *Mon. Not. Roy. Astron. Soc.* 145:271–295.

Larson, R. B. 1985. Cloud fragmentation and stellar masses. *Mon. Not. Roy. Astron. Soc.* 214:379–398.

Launhardt, R., Mezger, P. G., Haslam, C. G. T., Kreysa, E., Lemke, R., Sievers, A., and Zylka, R. 1996. Dust emission from star-forming regions. IV. Dense cores in the Orion B molecular cloud. *Astron. Astrophys.* 312:569–584.

Lay, O. P., Carlstrom, J. E., and Hills, R. E. 1995. NGC 1333 IRAS 4: Further multiplicity revealed with the CSO-JCMT interferometer. *Astrophys. J. Lett.* 452:L73–L76.

Lee, C. W, and Myers, P. C. 1999. A catalogue of optically selected cores. *Astrophys. J. Suppl.* 123:333.
Lefloch, B., Eislöffel, J., Lazareff, B. 1996. The remarkable Class 0 source Cep E. *Astron. Astrophys.* 313:L17–L20.
Lefloch, B., Castets, A., Cernicharo, J., and Loinard, L. 1998. Widespread SiO emission in NGC1333. *Astrophys. J. Lett.* 504:L109–L112.
Lehtinen, K. 1997. Spectroscopic evidence of mass infall towards an embedded infrared source in the globule DC 303.8-14.2. *Astron. Astrophys.* 317:L5–L8.
Leous, J. A., Feigelson, E. D., André, P., and Montmerle, T. 1991. A rich cluster of radio stars in the Rho Ophiuchi cloud cores. *Astrophys. J.* 379:683–688.
Li, Z.-Y. 1998. Formation and collapse of magnetized spherical molecular cloud cores. *Astrophys. J.* 493:230–246.
Li, Z.-Y., and Shu, F. H. 1996. Magnetized singular isothermal toroids. *Astrophys. J.* 472:211–224.
Li, Z.-Y., and Shu, F. H. 1997. Self-similar collapse of an isopedic isothermal disk. *Astrophys. J.* 475:237–250.
Looney, L. W., Mundy, L. G., and Welch, W. J. 1999. Unveiling the envelope and disk: A sub-arcsecond survey of circumstellar structures. *Astrophys. J.,* in press.
Lucas, P. W., and Roche, P. F. 1997. Butterfly star in Taurus: Structures of young stellar objects. *Mon. Not. Roy. Astron. Soc.* 286:895–919.
Mardones, D., Myers, P. C., Tafalla, M., Wilner, D. J., Bachiller, R., Garay, G. 1997. A search for infall motions toward nearby young stellar objects. *Astrophys. J.* 489:719–733.
Mauersberger, R., Wilson, T. L., Mezger, P. G., Gaume, R., Johnston, K. J. 1992. The internal structure of molecular clouds. III. Evidence for molecular depletion in the NGC 2024 condensations. *Astron. Astrophys.* 256:640–651.
McCaughrean, M. J., Rayner, J. T., and Zinnecker, H. 1994. Discovery of a molecular hydrogen jet near IC 348. *Astrophys. J.* 436:L189–L192.
McKee, C. F. 1989. Photoionization-regulated star formation and the structure of molecular clouds. *Astrophys. J.* 345:782–801.
McLaughlin, D. E., and Pudritz, R. E. 1997. Gravitational collapse and star formation in logotropic and nonisothermal spheres *Astrophys. J.* 476:750–765.
McMullin, J. P., Mundy, L. G., Wilking, B. A., Hezel, T., and Blake, G. A. 1994. Structure and chemistry in the northwestern condensation of the Serpens molecular cloud core. *Astrophys. J.* 424:222–236.
Men'shchikov, A. B., and Henning, T. 1997. Radiation transfer in circumstellar disks. *Astron. Astrophys.* 318:879–907.
Menten, K. M., Serabyn, E., Güsten, R., and Wilson, T. L. 1987. Physical conditions in the IRAS 16293-2422 parent cloud. *Astron. Astrophys.* 177:L57–L60.
Mezger, P. G., Sievers, A. W., Haslam, C. G. T., Kreysa, E., Lemke, R., Mauersberger, R., and Wilson, T. L. 1992. Dust emission from star forming regions. II. The NGC 2024 cloud core: Revisited. *Astron. Astrophys.* 256:631–639.
Mizuno, A., Fukui, Y., Iwata, T., Nozawa, S., Takana, T. 1990. A remarkable multilobe molecular outflow: Rho Ophiuchi East, associated with IRAS 16293-2422. *Astrophys. J.* 356:184–194.
Mizuno, A., Onishi, T., Hayashi, M. Ohashi, N., Sunada, K., Hasegawa, T., and Fukui, Y. 1994. Molecular cloud condensation as a tracer of low-mass star formation. *Nature* 368:719–721.
Molinari, S., Testi, L., Brand, J., Cesaroni, R., and Palla, F. 1998. IRAS 23385 +6053: A prototype massive Class 0 object. *Astrophys. J. Lett.* 505:L39–L42.
Moreira, M. C., Yun, J. L., Vázquez, R., and Torrelles, J. M. 1997. Thermal radio sources in Bok globules. *Astron. J.* 113:1371–1374.
Moriarty-Schieven, G. H., Wannier, P. G., Keene, J., Tamura, M. 1994. Circumprotostellar environments. 2: Envelopes, activity, and evolution. *Astrophys. J.* 436:800–806.

Motte, F. 1998. Structure des coeurs denses proto-stellaires: Étude en continuum millimétrique. Ph.D. Dissertation, University of Paris, XI.

Motte, F., André, P., and Neri, R. 1998. The initial conditions of star formation in the $\rho$ Ophiuchi main cloud: Wide-field millimeter continuum mapping. *Astron. Astrophys.* 336:150–172.

Motte, F. and André, P. 1999. Density structure of isolated protostellar envelopes: A millimeter continuum survey of Taurus infrared protostars. *Astron. Astrophys.,* in preparation.

Mouschovias, T. Ch. 1991. Single-stage fragmentation and a modern theory of star formation. In *The Physics of Star Formation and Early Stellar Evolution,* ed. C. J. Lada and N. D. Kylafis (Dordrecht: Kluwer), pp. 449–468.

Mouschovias, T. Ch. 1995. Role of magnetic fields in the early stages of star formation. In *The Physics of the Interstellar Medium and Intergalactic Medium,* ed. A. Ferrara, C. F. McKee, C. Heiles, and P. R. Shapiro (San Francisco: Astronomical Society of the Pacific), 80:184–217.

Mundy, L. G., Wootten, H. A., Wilking, B. A., Blake, G. A., and Sargent, A. I. 1992. IRAS 16293-2422: A very young binary system? *Astrophys. J.* 385:306–313.

Mundy, L. G., McMullin, J. P., and Grossman, A. W. 1993. Observations of circumstellar disks at centimeter wavelengths. *Icarus* 106:11–19.

Myers, P. C. 1998. Cluster-forming molecular cloud cores. *Astrophys. J. Lett.* 496:L109–L112.

Myers, P. C., and Benson, P. J. 1983. Dense cores in dark clouds. II. $NH_3$ observations and star formation. *Astrophys. J.* 266:309–320.

Myers, P. C., and Fuller, G. A. 1993. Gravitational formation times and stellar mass distributions for stars of mass 0.3–30 $M_\odot$. *Astrophys. J.* 402:635–642.

Myers, P. C., and Ladd, E. F. 1993. Bolometric temperatures of young stellar objects. *Astrophys. J. Lett.* 413:L47–L50.

Myers, P. C., Fuller, G. A., Mathieu, R. D., Beichman, C. A., Benson, P. J., Schild, R. E., and Emerson, J. P. 1987. Near-infrared and optical observations of IRAS sources in and near dense cores. *Astrophys. J.* 319:340–357.

Myers, P. C., Bachiller, R., Caselli, P., Fuller, G. A., Mardones, D., Tafalla, M., and Wilner, D. J. 1995. Gravitational infall in the dense cores L1527 and L483. *Astrophys. J. Lett.* 449:L65–L68.

Myers, P. C., Adams, F. C., Chen, H., and Schaff, E. 1998. Evolution of the bolometric temperature and luminosity of young stellar objects. *Astrophys. J.* 492:703–726.

Myhill, E. A., and Kaula, W. M. 1992. Numerical models for the collapse and fragmentation of centrally condensed molecular cloud cores. *Astrophys. J.* 386:578–586.

Nakano, T. 1984. Contraction of magnetic interstellar clouds. *Fund. Cosm. Phys.* 9:139–231.

Nakano, T. 1998. Star formation in magnetic clouds. *Astrophys. J.* 494:587–604.

Ohashi, N., Hayashi, M., Ho, P. T. P., and Momose, M. 1997. Interferometric imaging of IRAS 04368+2557 in the L1527 molecular cloud core: A dynamically infalling envelope with rotation. *Astrophys. J.* 475:211–223.

O'Linger, J., Wolf-Chase, G. A., Barsony, M., and Ward-Thompson, D. 1999. L1448 IRS2: A HIRES-Identified Class 0 protostar. *Astrophys. J.* 515:696–705.

Ossenkopf, V., and Henning, T. 1994. Dust opacities for protostellar cores. *Astron. Astrophys.* 291:943–959.

Ouyed, R., and Pudritz, R. E. 1997. Numerical simulations of astrophysical jets from Keplerian disks. I. Stationary models. *Astrophys. J.* 482:712–732.

Padoan, P., Nordlund, A., and Jones, B. J. T. 1997. The universality of the stellar initial mass function. *Mon. Not. Roy. Astron. Soc.* 288:145–152.

Palla, F., and Stahler, S. W. 1991. The evolution of intermediate-mass protostars. I. Basic results. *Astrophys. J.* 375:288–299.

Parker, N. D., Padman, R., and Scott, P. F. 1991. Outflows in dark clouds. Their role in protostellar evolution. *Mon. Not. Roy. Astron. Soc.* 252:442–461.

Persi, P., Ferrari-Toniolo, M., Marenzi, A. R., Anglada, G., Chini, R., Krügel, E., and Sepulveda, I. 1994. Infrared images, 1.3 mm continuum and ammonia line observations of IRAS 08076-3556. *Astron. Astrophys.* 282:233–239.

Phelps, R., and Barsony, M. 2000. Herbig-Haro objects in Serpens and Ophiuchus. *Astron. J.,* in preparation.

Pollack, J. B., Hollenbach, D., Beckwith, S., Simonelli, D. P., Roush, T., and Fong, W. 1994. Composition and radiative properties of grains in molecular clouds and accretion disks. *Astrophys. J.* 421:615–639.

Pravdo, S. H., Rodríguez, L. F., Curiel, S., Cantó, J., Torrelles, J. M., Becker, R. H., and Sellgren, K. 1985. Detection of radio continuum emission from Herbig-Haro objects 1 and 2 and from their central exciting source. *Astrophys. J. Lett.* 293:L35–L38.

Preibisch, Th., Ossenkopf, V., Yorke, H. W., and Henning, Th. 1993. The influence of ice-coated grains on protostellar spectra. *Astron. Astrophys.* 279:577–588.

Pringle, J. E. 1989. On the formation of binary stars. *Mon. Not. Roy. Astron. Soc.* 239:361–370.

Pudritz, R. E., Wilson, C. D., Carlstrom, J. E., Lay, O. P., Hills, R. E., and Ward-Thompson, D. 1996. Accretions disks around Class 0 protostars: The case of VLA 1623. *Astrophys. J. Lett.* 470:L123–L126.

Reipurth, B., Chini, R., Krügel, E., Kreysa, E., and Sievers, A. 1993. Cold dust around Herbig-Haro energy sources: A 1300 $\mu$m survey. *Astron. Astrophys.* 273:221–238.

Reipurth, B., Nyman, L.-A., and Chini, R. 1996. Protostellar candidates in southern molecular clouds. *Astron. Astrophys.* 314:258–264.

Richer, J. S., Hills, R. E., and Padman, R. 1992. A fast CO jet in Orion B. *Mon. Not. Roy. Astron. Soc.* 254:525–538.

Richer, J. S., Padman, R., Ward-Thompson, D., Hills, R. E., and Harris, A. I. 1993. The molecular environment of S106 IR. *Mon. Not. Roy. Astron. Soc.* 262:839–854.

Ristorcelli, I., Serra, G., Lamarre, J. M., et al. 1998. Discovery of a cold extended condensation in the Orion A complex. *Astrophys. J.* 496:267–273.

Safier, P. N., McKee, C. F., and Stahler, S. W. 1997. Star formation in cold, spherical, magnetized molecular clouds. *Astrophys. J.* 485:660–679.

Sandell, G. 1994. Secondary calibrators at submillimeter wavelengths. *Mon. Not. Roy. Astron. Soc.* 262:839–854.

Sandell, G., and Weintraub, D. A. 1994. A submillimeter protostar near LkH-alpha 198. *Astron. Astrophys.* 292:L1–L4.

Sandell, G., Aspin, C., Duncan, W. D., Russell, A. P. G., and Robson, E. I. 1991. NGC 1333 IRAS 4. A very young, low-luminosity binary system. *Astrophys. J.* 376:L17–L20.

Sandell, G., Knee, L. B. G., Aspin, C., Robson, I. E., and Russell, A. P. G. 1994. A molecular jet and bow shock in the low mass protostellar binary NGC 1333-IRAS2. *Astron. Astrophys.* 285:L1–L4.

Sandell, G., Avery, L. W., Baas, F., Coulson, I., Dent, W. R. F., Friberg, P., Gear, W. P. K., Greaves, J., Holland, W., Jenness, T., Jewell, P., Lightfoot, J., Matthews, H. E., Moriarty-Schieven, G., Prestage, R., Robson, E. I., Stevens, J., Tilanus, R. P. J., and Watt, G. D. 1999. A jet-driven, extreme high-velocity outflow powered by a cold, low-luminosity protostar near NGC 2023. *Astrophys. J.,* 519:236–243.

Saraceno, P., André, P., Ceccarelli, C., Griffin, M., and Molinari, S. 1996*a*. An evolutionary diagram for young stellar objects. *Astron. Astrophys.* 309:827–839.

Saraceno, P., D'Antona, F., Palla, F., Griffin, M., and Tommasi, E. 1996*b*. The luminosity-mm flux correlation of Class I sources exciting outflows. In *The Role of Dust in the Formation of Stars,* ed. H. U. Käufl and R. Siebenmorgen (Berlin: Springer), pp. 59–62.

Scalo, J. 1998. The IMF revisited: A case for variations. In *The Stellar Initial Mass Function,* ASP Conf. Ser. 142, ed. G. Gilmore and D. Howell (San Francisco: Astronomical Society of the Pacific), pp. 201–236.

Shu, F. H. 1977. Self-similar collapse of isothermal spheres and star formation. *Astrophys. J.* 214:488–497.

Shu, F. H., Adams, F. C., and Lizano, S. 1987. Star formation in molecular clouds. Observation and theory. *Ann. Rev. Astron. Astrophys.* 25:23–81.

Shu, F., Najita, J., Galli, D., Ostriker, E., and Lizano S. 1993. The collapse of clouds and the formation and evolution of stars and disks. In *Protostars and Planets III,* ed. E. H. Levy and J. I. Lunine (Tucson: University of Arizona Press), pp. 3–45.

Shu, F. H., Najita, J., Ostriker, E., Wilkin, F., Ruden, S., and Lizano, S. 1994. Magnetocentrifugally driven flows from young stars and disks. I. A generalized model. *Astrophys. J.* 429:781–796.

Silk, J. 1995. A theory for the initial mass function. *Astrophys. J. Lett.* 438:L41–L44.

Sonnhalter, C., Preibisch, T., and Yorke, H. W. 1995. Frequency dependent radiation transfer in protostellar disks. *Astron. Astrophys.* 299:545–556.

Stahler S. W. 1988. Deuterium and the stellar birthline. *Astrophys. J.* 332:804–825.

Stahler, S. W., and Walter, F. M. 1993. Pre-main-sequence evolution and the birth population. In *Protostars and Planets III,* ed. E. H. Levy and J. I. Lunine (Tucson: University of Arizona Press), pp. 405–428.

Stanke, T., McCaughrean, M., and Zinnecker, H. 1998. First results of an unbiased $H_2$ survey for protostellar jets in Orion A. *Astron. Astrophys.* 332:307–313.

Tafalla, M., Mardones, D., Myers, P. C., Caselli, P., Bachiller, R., and Benson, P. J. 1998. L1544: A starless dense core with extended inward motions. *Astrophys. J.* 504:900–914.

Tamura, M., Hayashi, S. S., Yamashita, T., Duncan, W. D., and Hough, J. H. 1993. Magnetic field in a low-mass protostar disk. Millimeter polarimetry of IRAS 16293-2422. *Astrophys. J. Lett.* 404:L21–L24.

Terebey, S., and Padgett, D. L. 1997. Millimeter interferometry of Class 0 sources: Rotation and infall towards L1448N. In *Herbig-Haro Flows and the Birth of Low Mass Stars,* IAU Symp. 182, ed. B. Reipurth and C. Bertout (Dordrecht: Kluwer), pp. 507–514.

Terebey, S., Vogel S. N., Myers P. C. 1989. High-resolution CO observations of young low-mass stars. *Astrophys. J.* 340:472–478.

Terebey, S., Chandler, C. J., and André, P. 1993. The contribution of disks and envelopes to the millimeter continuum emission from very young low-mass stars. *Astrophys. J.* 414:759–772.

Testi, L., and Sargent, A. I. 1998. Star formation in clusters: A survey of compact millimeter-wave sources in the Serpens core. *Astrophys. J. Lett.* 508:L91–L94.

Tinney, C. G. 1993. The faintest stars: The luminosity and mass functions at the bottom of the main sequence. *Astrophys. J.* 414:279–301.

Tinney, C. G. 1995. The faintest stars: The luminosity and mass functions at the bottom of the main sequence: Erratum. *Astrophys. J.* 445:1017.

Tomisaka, K. 1996. Accretion in gravitationally contracting clouds. *Publ. Astron. Soc. Japan* 48:L97–L101.

Umemoto, T., Iwata, T., Fukui, Y., Mikami, H., Yamamoto, S., Kameyama, O., and Hirano, N. 1992. The outflow in the L1157 dark cloud: Evidence for shock heating of the interacting gas. *Astrophys. J. Lett.* 392:L83–L86.

Velusamy, T., and Langer, W. D. 1998. Outflow-infall interactions as a mechanism for terminating accretion in protostars. *Nature* 392:685–687.

Walker, C. K., Adams, F. C., and Lada, C. J. 1990. 1.3 millimeter continuum observations of cold molecular cloud cores. *Astrophys. J.* 349:515–528.

Walker, C. K., Lada, C. J., Young, E. T., Maloney, P. R., and Wilking, B. A. 1986. Spectroscopic evidence for infall around an extraordinary IRAS source in Ophiuchus. *Astrophys. J. Lett.* 309:L47–L51.

Walker, C. K., Narayanan, G., and Boss, A. P. 1994. Spectroscopic signatures of infall in young protostellar systems. *Astrophys. J.* 431:767–782.

Ward-Thompson, D. 1996. The formation and evolution of low mass protostars. *Astrophys. Space Sci.* 239: 151–170.

Ward-Thompson, D., Scott, P. F., Hills, R. E., and André, P. 1994. A submillimetre continuum survey of pre-protostellar cores. *Mon. Not. Roy. Astron. Soc.* 268:276–290.

Ward-Thompson, D., Chini, R., Krugel, E., André, P., and Bontemps, S. 1995*a*. A submillimetre study of the Class 0 protostar HH24MMS. *Mon. Not. Roy. Astron. Soc.* 274:1219–1224.

Ward-Thompson, D., Eiroa, C., and Casali, M. M. 1995*b*. Confirmation of the driving source of the NGC 2264G bipolar outflow: A Class 0 protostar. *Mon. Not. Roy. Astron. Soc.* 273:L25–L28.

Ward-Thompson, D., Buckley, H. D., Greaves, J. S., Holland, W. S., and André, P. 1996. Evidence for protostellar infall in NGC 1333-IRAS2. *Mon. Not. Roy. Astron. Soc.* 281:L53–L56.

Ward-Thompson, D., Motte, F., and André, P. 1999. The initial conditions of isolated star formation. III: Millimetre continuum mapping of prestellar cores. *Mon. Not. Roy. Astron. Soc.* 305:143–150.

White, G. J., Casali, M. M., and Eiroa, C. 1995. High resolution molecular line observations of the Serpens Nebula. *Astron. Astrophys.* 298:594–605.

Whitney, B. A., and Hartmann, L. 1993. Model scattering envelopes of young stellar objects. II: Infalling envelopes. *Astrophys. J.* 402:605–622.

Whitworth, A., and Summers, D. 1985. Self-similar condensation of spherically symmetric self-gravitating isothermal gas clouds. *Mon. Not. Roy. Astron. Soc.* 214:1–25.

Whitworth, A. P., Bhattal, A. S., Francis, N., and Watkins, S. J. 1996. Star formation and the singular isothermal sphere. *Mon. Not. Roy. Astron. Soc.* 283:1061–1070.

Wiesemeyer, H. 1997. The spectral signature of accretion in low-mass protostars. Ph. D. Dissertation, University of Bonn.

Wiesemeyer, H., Güsten, R., Wink, J. E., and Yorke, H. W. 1997. High resolution studies of protostellar condensations in NGC 2024. *Astron. Astrophys.* 320:287–299.

Wiesemeyer, H., Güsten, R., Cox, P., Zylka, R., and Wright, M. C. H. 1998. The pivotal onset of protostellar collapse: ISO's view and complementary observations. In *Star Formation with ISO,* ASP Conf. Ser. 132, ed. J. L. Yun and R. Liseau (San Francisco: Astronomical Society of the Pacific), pp. 189–194.

Wilking, B. A., Lada, C. J., and Young, E. T. 1989. IRAS observations of the Rho Ophiuchi infrared cluster: Spectral energy distributions and luminosity function. *Astrophys. J.* 340:823–852.

Wilking, B. A., Schwartz, R. D., Fanetti, T. M., and Friel, E. D. 1997. Herbig-Haro objects in the $\rho$ Ophiuchi cloud. *Publ. Astron. Soc. Pacific* 109:549–553.

Wilner, D. J., Welch, W. J., and Forster, J. R. 1995. Sub-arcsecond Imaging of W3(OH) at 87.7 GHz. *Astrophys. J. Lett.* 449:L73–L76.

Wolf-Chase, G. A., Barsony, M., Wootten, H. A., Ward-Thompson, D., Lowrance, P. J., Kastner, J. H., and McMullin, J. P. 1998. The Protostellar Origin of a CS Outflow in S68N. *Astrophys. J. Lett.* 501:L193–L198.

Wood, D. O. S., Myers, P. C., and Daugherty, D. A. 1994. IRAS images of nearby dark clouds. *Astrophys. J. Sup.* 95:457–501.

Wootten, A. 1989. The duplicity of IRAS 16293-2422: A protobinary star? *Astrophys. J.* 337:858–864.

Yorke, H. W., Bodenheimer, P., and Laughlin, G. 1995. The formation of protostellar disks. II: Disks around intermediate-mass stars *Astrophys. J.* 443:199–208.

Yu, K. C., Bally, J., and Devine, D. 1997. Shock-excited $H_2$ flows in OMC-2 and OMC-3. *Astrophys. J. Lett.* 485:L45–L48.

Yun, J. L., Moreira, M. C., Torrelles, J. M., Afonso, J. M., and Santos, N. C. 1996. A search for radio continuum emission from young stellar objects in Bok globules. *Astron. J.* 111:841–845.

Zavagno, A., Molinari, S., Tommasi, E., Saraceno, P., and Griffin, M. 1997. Young stellar objects in Lynds 1641: A submillimetre continuum study. *Astron. Astrophys.* 325:685–692.

Zhou, S., Evans, N. J., II, Kömpe, C., and Walmsley, C. M. 1993. Evidence for protostellar collapse in B335. *Astrophys. J.* 404:232–246.

Zinnecker, H., Bastien, P., Arcoragi, J. P., and Yorke, H. W. 1992. Submillimeter dust continuum observations of three low luminosity protostellar IRAS sources. *Astron. Astrophys.* 265:726–732.

Zinnecker, H., McCaughrean, M. J., and Rayner, J. T. 1998. A symmetrically pulsed jet of gas from an invisible protostar in Orion. *Nature* 394:862–865.